



1 **Overview towards improved understanding of the mechanisms leading to heavy**
2 **precipitation in the Western Mediterranean: lessons learned from HyMeX**

3

4 ^{1,2}Samira Khodayar, ³Silvio Davolio, ⁴Paolo Di Girolamo, ⁵Cindy Lebeaupin Brossier,
5 ⁶Emmanouil Flaounas, ⁵Nadia Fourrie, ^{7,8} Keun-Ok Lee, ⁵Didier Ricard, ⁵Benoit Vie,
6 ⁵Francois Bouttier, ²Alberto Caldas-Alvarez, ⁵Veronique Ducrocq

7

8 ¹Mediterranean Centre for Environmental Studies (CEAM), Valencia, Spain

9 ²Institute of Meteorology and Climate Research (IMK-TRO), Karlsruhe Institute of Technology (KIT),
10 Karlsruhe, Germany

11 ³National Research Council of Italy, Institute of Atmospheric Sciences and Climate, (CNR-ISAC), Bologna,
12 Italy

13 ⁴Scuola di Ingegneria, Università degli Studi della Basilicata (SI-UNIBAS), Potenza, Italy

14 ⁵CNRM, Université de Toulouse, Météo-France, CNRS, Toulouse, France

15 ⁶Institute of Oceanography, Hellenic Centre for Marine Research (HCMR), Athens, Greece

16 ⁷Laboratoire d'Aérodynamique, Université de Toulouse, CNRS, UPS, Toulouse, France

17 ⁸Laboratoire de L'Atmosphère et des Cyclones, UMR 8105 (CNRS, Université de La Réunion, Météo-
18 France), Saint Denis, France

19

20

21

22

23

24

25 * Corresponding author. E-mail address: khodayar_sam@gva.es (S. Khodayar)

26 Mediterranean Centre for Environmental Studies (CEAM),

27 Technological Park, Charles R. Darwin Street, 14 46980 - Paterna - Valencia - Spain



28 **Abstract**

29 Heavy precipitation (HP) constitutes a major meteorological threat in the western
30 Mediterranean (WMed). Every year, recurrent events affect the area with fatal
31 consequences on infrastructure and personal losses. Despite this being a well-known
32 issue, widely investigated in the past, still open questions remain. Particularly, the
33 understanding of the underlying mechanisms and the modelling representation of the
34 events must be improved. One of the major goals of the Hydrological cYcle in the
35 Mediterranean eXperiment (HyMeX; 2010-2020) has been to advance knowledge on this
36 topic. In this article we present an overview of the most recent lessons learned from
37 HyMeX towards improved understanding of the mechanisms leading to HP in the WMed.

38 The unique network of instruments deployed, the use of finer model resolutions and of
39 coupled models, provided an unprecedented opportunity to validate numerical model
40 simulations, to develop improved parameterizations, designing high-resolution ensemble
41 modelling approaches and sophisticated assimilation techniques across scales.

42 All in all, HyMeX and particularly the science team heavy precipitation favoured the
43 evidencing of theoretical results, the enrichment of our knowledge on the genesis and
44 evolution of convection in a complex topography environment, and the improvement of
45 precipitation forecasts. Illustratively, the intervention of cyclones and warm conveyor
46 belts in the occurrence of heavy precipitation has been pointed out, the crucial role of
47 the spatio-temporal distribution of the atmospheric water vapor for the understanding
48 and accurate forecast of the timing and location of deep convection has been evidenced,
49 as well as the complex interaction among processes across scales. The importance of
50 soil and ocean conditions and the interactions among systems were highlighted and such
51 systems were specifically developed in the framework of HyMeX to improve the realism
52 of weather forecasts. Furthermore, the benefits of cross-disciplinary efforts within HyMeX
53 have been a key asset in bringing a step forward our knowledge about heavy
54 precipitation in the Mediterranean region.

55

56

57

58

59



1. Introduction and Motivation

A 10-Year Multidisciplinary Program on the Mediterranean Water Cycle, HyMeX, Hydrological Cycle in the Mediterranean Experiment (Drobinski et al., 2014), has come to an end (2010-2020). With the main goal to advance the scientific knowledge of the Mediterranean water cycle variability and to improve the process-based and regional climate models, different temporal scales are considered, from weather-scale to the seasonal and interannual scales. Special focus is put on the hydrometeorological extremes and consequent social and economic impacts, as well as the vulnerability and the adaptation capacity of the Mediterranean population under Climate Change.

The unique character of the Mediterranean basin and surrounding countries resulting from the geographical location, climatic conditions, and topography, makes the region prone to extreme phenomena; heavy precipitation and flash floods, as well as heat waves and drought (e.g., Mariotti, 2010). The region, defined as one of the two main “hot spots” of climate change (Giorgi, 2006; IPCC, 2013), is in a transition area, therefore, very sensitive to global climate change at short and long-time scales. An increase in interannual rainfall variability, strong warming and drying in addition to a significant population growth are projected for the coming future. Despite the overall Mediterranean climate drying, under climate change, intensity of heavy precipitation events (HPEs) is expected to increase (Planton et al., 2016; Jacob et al., 2013; Drobinski et al., 2016; Colmet-Daage et al., 2017; Trambly and Somot, 2018; Giorgi et al., 2019). In this context, threats posed from the expected increase in frequency and intensity of events conducive to floods and droughts (Gao et al., 2006; Orłowsky and Seneviratne, 2011) are seen with great concern. Countries surrounding the Mediterranean basin already suffer water problems in relation to water shortages and floods. Food security could also become an issue (Nelson et al., 2010).

HPEs and the associated flash floods are the most dangerous meteorological hazards affecting the Mediterranean countries in terms of mortality, and hundreds of millions of euros in damages are registered every year (Llasat et al., 2010, 2013; Doocy et al., 2013). The Mediterranean basin and particularly the surrounding mountainous coastal regions are often affected by these phenomena, regularly in the autumn period. The Mediterranean Sea, acting as a heat and moisture source, and the steep orography, triggering convection, are key aspects determining the occurrence of heavy precipitation in the region which is mainly of convective nature (Funatsu et al., 2008; Dayan et al., 2015). Rainfall accumulations greater than 100-150 mm may be expected in less than a day or even just a few hours resulting mostly from quasi-stationary mesoscale convective



97 systems (MCSs; Lee et al., 2018, 2017, 2016; Duffourg et al 2018; Buzzi et al., 2014).
98 Such rainfall accumulations are favoured by a slowly evolving synoptic situation,
99 characterized by an upper-level trough and consequent cyclogenesis that induces
100 advection of warm and moist air from the Mediterranean Sea (Duffourg and Ducrocq,
101 2011) to the coasts through marine low-level jets (Homar et al., 1999; Jansa et al., 2001;
102 Nuissier et al., 2011; Ricard et al., 2012; Khodayar et al., 2016b). Strong wind with high
103 sea surface temperature (SST) governs evaporation, which moistens and warms the
104 lowest levels of the atmosphere, thus increasing instability and finally often enhancing
105 the convection intensity (Xie et al., 2005, Lebeaupin et al., 2006; Stocchi and Davolio,
106 2017, Rainaud et al., 2017; Senatore et al., 2020a). Low-level convergence over the sea,
107 cold pools beneath the convective systems, or topographic lifting when encountering the
108 coastal mountains trigger deep convection, forcing the lift of the conditionally unstable
109 low-level flow. The synoptic-scale situations associated with these episodes are
110 generally well-known and well represented in numerical weather prediction (NWP) model
111 simulations. However, the accuracy of forecasts is still insufficient to adequately assess
112 timing, location and intensity of rainfall and flash flooding in certain situations, which is a
113 key step towards prevention and mitigation. This is mostly in relation to (a) model
114 limitations in terms of predictability of small-scale processes (e.g., convection,
115 turbulence) and feedbacks (e.g., soil, atmosphere, ocean) and their non-linear
116 interaction across scales, (b) lack of knowledge regarding underlying mechanisms, and
117 (c) absence of adequate observations to help us advance our understanding and
118 improving model capabilities.

119 This issue is one of the main objectives of the HyMeX international programme, and of
120 its associated first special observation period (SOP1; Ducrocq et al., 2014), from 5
121 September to 6 November 2012, dedicated to heavy precipitation and flash flooding.
122 Because of the large number of instruments deployed, the unprecedented high spatial-
123 temporal coverage achieved and the quality of the derived observations, the SOP1 has
124 offered a unique opportunity to improve understanding and advance documenting high-
125 impact weather events. This is in addition to the significant progress achieved in the last
126 decade through the development of convection-permitting models, whose benefit has
127 been sufficiently demonstrated (Richard et al., 2007; Fosser et al., 2014, Prein et al.,
128 2015; Clark et al, 2016, among others) and it is widely used nowadays from the scientific
129 community.

130 The major goal of this article is to expose an overview on some of the recent years' main
131 achievements towards better understanding of the mechanisms leading to heavy
132 precipitation in the WMed in the framework of the HyMeX international programme.
133 Advances regarding improved understanding of the mechanisms governing the initiation



134 and intensification of precipitating systems producing large amounts of rainfall are
135 thoroughly discussed in terms of in situ observations and high-resolution modelling
136 systems, as well as the synergetic use of both to help us bridging knowledge gaps. An
137 intensive observation period IOP16, which took place during the SOP1, is taken as a
138 paradigm to illustrate some of the main HyMeX results in the field of heavy precipitation.
139 This paper is structured as follows: in section 2 we describe the general conditions
140 leading to HP during the SOP1 period, the state-of-the-art of the observational networks
141 deployed in this time, as well as the modelling strategy developed. Additionally, the
142 IOP16, which has been used throughout the paper for illustrating some of the results is
143 presented. In section 3, the main advances regarding HP understanding and modelling
144 are presented, including the large-scale dynamics, advances in moist process
145 understanding, low-level dynamics, the impacts of the land and the sea surfaces and
146 microphysics. Section 4 is devoted to the examination of the improvements in the multi-
147 scale modelling of HP and in section 5 some conclusions and recommendations are
148 summarized.

149

150 **2. Heavy precipitation during the HyMeX SOP1 period**

151 The SOP1 campaign took place in 2012, from 5 September to 6 November, when the
152 probability of HPE occurrence in the north-western Mediterranean is the highest. About
153 30% of the days in this period experienced, indeed, rainfall accumulations over 100 mm
154 somewhere in the investigation domain. Sixteen Intensive Observation Periods (IOPs)
155 were launched during the campaign, most of them occurring in the period after mid-
156 October to the end of the SOP1 (Ducrocq et al., 2014). This agrees with the monthly
157 precipitation totals being close to the climatological values in September, but well above
158 in October (Khodayar et al., 2016b). Most IOPs did not affect a single site but
159 encompassed several regions of the north-western Mediterranean. The most affected
160 sites were the Cévennes-Vivarais (CV), including the Massif Central and the French
161 Southern Alps, as well as the Liguria-Tuscany (LT) region in Italy.

162 **2.1. State-of-the-art observational capabilities and modelling activities**

163 More than 200 research instruments were deployed over the WMed Sea and surrounding
164 countries, namely Spain, France, and Italy to ensure a close observation of the
165 precipitating systems and a fine-scale survey of the upstream meteorological conditions
166 over the Mediterranean. Ducrocq et al. (2014) provides a comprehensive description of
167 the observing systems deployed during the SOP1. Furthermore, this unique network of
168 instruments provided an unprecedented opportunity to validate more accurately NWP
169 model simulations, to develop novel data assimilation techniques and to improve model



170 parameterizations with the purpose of better predicting the evolution of the environment
171 across scales.

172 **2.1.1 Ground-based, airborne, and seaborne observations**

173 One unique aspect of HyMeX-SOP1 was represented by the availability of a large
174 ensemble of ground-based and airborne instruments, covering a major portion of the
175 WMed and its surrounding coastal regions in France, Italy, and Spain. The observational
176 domain of HyMeX-SOP1 was defined to include the area with the highest occurrence of
177 HPEs and being within the ranges of aircraft flight endurance. Within this large domain,
178 five measurement sites including advanced research instruments were established, i.e.
179 the Cévennes-Vivarais (CV) and the Corsica (CO) sites, the Central Italy (CI) and
180 Northeastern Italy (NEI) sites, and the Spanish Balearic Islands (BA) site in Menorca
181 (Ducrocq et al., 2014). Most sites were equipped with soil moisture sensors, turbulence
182 or energy balance stations, microwave radiometers, lidars, radars (cloud, precipitation
183 and/or wind) and radiosonde launching facilities, in addition to the operational
184 meteorological and hydrological ground networks covering the entire SOP1 domain.
185 Thus, an unprecedented dense network of rain gauges was available over France, Italy,
186 and Spain, with a density of about one hourly rain gauge per 180 km². This network
187 operated in combination with a radar network including a variety of S-band, C-band
188 Doppler (two of them being polarimetric) and X-band radars (one of them being
189 polarimetric). A similarly dense network of Global Positioning System (GPS) stations was
190 also established, with stations covering the north-western Mediterranean basin and
191 including measurements from 25 European, national, and regional GPS networks (Bock
192 et al., 2016).

193 Three aircrafts participated in the field campaign: the French ATR42, the French Falcon
194 20 (operated by SAFIRE (Service des Avions Français Instrumentés pour la Recherche
195 en Environnement)) and the German Do128 (Corsmeier et al., 2001). The ATR42
196 involvement was primarily aimed to characterize the origin and transport pattern of water
197 vapor and aerosol in pre-convective conditions and their link with heavy precipitating
198 systems. Its main payload was the airborne dial LEANDRE 2, capable of profiling water
199 vapor mixing ratio above or beneath the aircraft. The F20 aircraft primary mission was
200 the characterization of the microphysical and kinematic processes taking place within
201 convective precipitating systems, this objective being pursued based on the use of
202 advanced microphysical in situ probes and the 95-GHz Doppler cloud radar RASTA
203 (Radar Aéroporté et Sol de Télédétection des propriétés nuAgeuses, Protat et al., 2009).
204 Furthermore, the German Do 128 research aircraft was equipped with fast sensors to
205 measure turbulent fluxes, water vapor inlet, and stable water isotope measurements
206 (Sodemann et al., 2017) with the primary goal of monitoring upstream low-level



207 conditions before and during HPEs and investigating the orographic and thermal impact
208 of the island on the initiation and evolution of diurnal convective activity.
209 During HyMeX-SOP1 Boundary Layer Pressurized Balloons (BLPBs) were also
210 launched from Menorca, flying at a nearly constant height (Doerenbecher et al., 2016)
211 and providing Lagrangian trajectories of specific humidity, temperature, pressure, and
212 horizontal wind.

213
214 Two ground-based Raman lidars were involved, namely the system BASIL (Di Girolamo
215 et al., 2009), deployed in Candillargues (Southern France) and the system WALI (Water-
216 vapour Raman Lidar; Chazette et al., 2016), deployed in Ciutadella (Menorca, Balearic
217 Islands). Both systems provided long-term records of high-resolution and accurate
218 humidity measurements, both in daytime and night-time, throughout the duration of
219 HyMeX-SOP1.

220
221 At sea, several platforms were deployed to monitor the ocean upper-layer and the
222 exchanges with the atmosphere (Ducrocq et al., 2014, Lebeaupin Brossier et al., 2014,
223 Rainaud et al., 2015). Two Météo-France moored buoys, LION (4.7°E–42.1°N) and
224 AZUR (7.8°E–43.4°N), routinely provide the 2 m-temperature, humidity, 10 m-wind
225 speed, direction and gust intensity, mean sea level pressure and sea surface parameters
226 (SST, wave height and period). They were equipped with additional sensors for HyMeX
227 with radiative flux measurements, raingauges, a thermosalinograph measuring the near-
228 surface temperature and salinity, and a thermobathymetric chain giving the ocean
229 temperature between 5 and 250 m-depth. During SOP1, up to five gliders monitored the
230 area simultaneously, providing 0–1000 m profiles along repeated transects.
231 Observations from ships include CTD profiles (up to 200 m-depth) and radiosoundings
232 from the port-tender Le Provence sent in the Gulf of Lion for 3 IOPs (IOP7, IOP12 and
233 IOP16). Finally, the freighter Marfret-Niolon that regularly linked Marseille (France) with
234 Algiers (Algeria), was equipped for HyMeX with the SEOS (Sea Embedded Observation
235 System; <http://dx.doi.org/10.6096/MISTRALS-HYMEX.748>) station, measuring air
236 temperature, relative humidity, pressure, wind and SST. Another sensor provided
237 measurements of sea temperature at almost 3 m-depth, using a high-quality temperature
238 probe (TRANSMED data: <http://dx.doi.org/10.6096/MISTRALS-HYMEX.973>), backed by
239 a thermosalinograph that also provided in-situ salinity.

240 **2.1.2 HyMeX modelling strategy**

241 Despite significant efforts to improve the skill of forecasts, the forecasting accuracy has
242 been proved still insufficient in terms of amount, timing, and location of heavy



precipitation. The design of the HyMeX modelling strategy considered three key issues proved to be relevant to reduce modelling uncertainty: (a) to be consistent with the observation strategy, (b) to integrate numerical models of the atmosphere, ocean, and land and (c) to include models of the climate system to cover all scales of time and space. Moreover, through the refinement of model grids and the development of convection-permitting NWP systems and Regional Climate Models (RCM), significant progress has been made to improve the simulations of HPEs, the knowledge of the relevant processes and their interactions across scales, as well as to reduce the large uncertainties on the future evolution under climate change. The use of finer-scale and coupled models representing more accurately the atmosphere-ocean-land systems and their interactions, and/or the detailed validation using the SOP1 measurements allowed the development of improved parameterizations of physical processes, the design of high-resolution ensemble modelling approaches with greater number of ensemble members, and a more sophisticated and efficient use of observations for assimilation purposes.

Profiting from these efforts, the HyMeX community has made relevant advances in process knowledge and prediction of heavy precipitation. Some of these advances are discussed and illustrated in the coming sections using the IOP16, which is introduced in the following.

2.2. Illustrative case: IOP 16

The IOP 16 is a well-documented and widely investigated event observed in the period 25-29 October 2012 over the WMed region. IOP 16 was one of the best equipped observational periods in terms of instrumental coverage during HyMeX-SOP1 (Figure 1). Most ground-based and air-borne instrumentation were successfully operational, providing high quality data, with almost all the on-demand SOP1 instruments involved. Benefiting from this large observational dataset, an extensive number of modelling activities focused on the IOP 16, with the purpose of investigating different issues related with the occurrence of heavy precipitation, such as the impact of the turbulence representation on the sensitivity of the simulated convective systems (Martinet et al., 2017), the underlying mechanisms of offshore deep convection initiation and maintenance (Duffourg et al., 2016), some assimilation or pre-assimilation experiments (Borderies et al., 2019a), the impact of fine-scale air-sea interactions and coupled processes on heavy precipitation (Rainaud et al., 2017), or novel Large Eddy Simulation (LES) of a HPE (Nuissier et al., 2020).

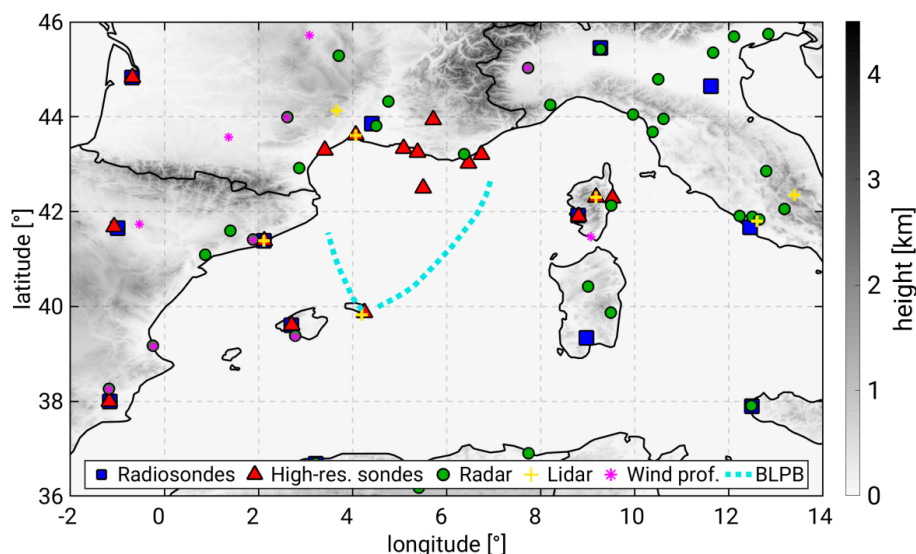
This event was associated with a propagating cyclone and was observed in two dedicated periods: (a) the IOP16a (25–26 October), characterized by heavy



278 precipitation over CV and LT, when several quasi-stationary MCSs developed, two of
279 them over the sea, with subsequent heavy precipitation over the French and Italian
280 coasts on 26 October 2012, and (b) the IOP16b (27–29 October) characterized by heavy
281 precipitation over CI, NEI, and CO regions.

282 The IOP16a was driven by the presence of a cyclone moving from the easternmost
283 Atlantic to the Pyrenees, followed in phase by a cut-off low, associated with upper-level
284 high potential vorticity values. In the lower troposphere, the cyclone provoked
285 southwesterly advection of moist and warm air above 20 °C. On the morning of the 26
286 October the cyclone was centered over the Pyrenees, forming a convergence line
287 between the southerly flow and the southwesterly colder winds, while over the Tyrrhenian
288 Sea a southerly moist and warm flow from Tunisia to the Gulf of Genoa established
289 (Fourrié et al., 2015). During the night from the 25th to the 26th of October and in the
290 following day several MCSs with quasi-stationary behavior formed within a “comma-
291 shaped” cloud coverage. First over the sea, between the eastern Spanish coast and the
292 Balearic Islands (Duffourg et al., 2016), afterwards over the Gulf of Lion inducing large
293 amounts of precipitation over sea during the morning. The first MCS split in two. One
294 system (MCS1a) moved towards the south east of the Massif Central, but progressively
295 decayed producing just orographic rainfall; the second (MCS1b) strengthened and
296 caused a large precipitation accumulation over the Var region during the afternoon,
297 nearly 150 mm in 24 h, causing two fatalities in the city of Toulon. A third MCS initiated
298 at about 06:00 UTC on the 26 October on the Italian coast of Liguria. The MCS
299 development occurred also offshore Sardinia and Corsica and reached central Italy
300 during the evening on 26 October, leading to 250 mm daily precipitation on this day over
301 Liguria-Tuscany, with local flash flooding. On the same day, over the Cévennes-Vivarais
302 region, daily precipitation reached 170 mm.

303 During the second period, 27–28 October 2012, the cyclone centre reached the lowest
304 pressure of 985 hPa over the Alps (Fig. 2), associated with a clear trough in the upper
305 troposphere and provoking severe northwesterly/northerly winds advecting cold and dry
306 air over the WMed Sea and inducing large evaporation and ocean cooling and mixing
307 (Lebeaupin Brossier et al., 2014; Rainaud et al., 2015, 2017; Seyfried et al., 2018). The
308 relationship between cyclone dynamics and heavy rainfall during IOP16 is discussed in
309 detail by Flaounas et al. (2015a).



310

311 **Figure 1:** Location of selected experimental setup during the IOP16, 25-28 Oct. 2012,
 312 including radiosondes and high-resolution sondes, radar, lidar, wind profilers, and
 313 Boundary Layer Pressurized Balloons (BLPB). The position of the GPS receivers can be
 314 found in Figure 3d.

315

316 **3. Towards improved understanding of the mechanisms leading to heavy** 317 **precipitation in the Western Mediterranean**

318 **3.1 Large-scale dynamics and HPE occurrence**

319 Mediterranean cyclogenesis is typically triggered by baroclinic instability because of
 320 Rossby wave breaking and the intrusion of upper tropospheric filaments of air masses
 321 of high potential vorticity over the Mediterranean (Grams et al., 2011; Raveh-Rubin and
 322 Flaounas, 2017). Therefore, most intense Mediterranean cyclones are baroclinic
 323 systems with frontal structures and associated airstreams such as dry air intrusions and
 324 warm conveyor belts (WCB; Ziv et al., 2009; Flaounas et al., 2015a). The latter
 325 corresponds to airstreams that ascend slantwise over the cyclone warm front and are
 326 responsible for the characteristic "comma-shaped" cloud coverage of mid-latitude
 327 storms. WCBs are associated with stratiform, but also with convective rainfall due to
 328 embedded convection within their large-scale ascent branch (Flaounas et al., 2018;
 329 Oertel et al., 2019). Such is the case of IOP16, where WCBs and deep convection

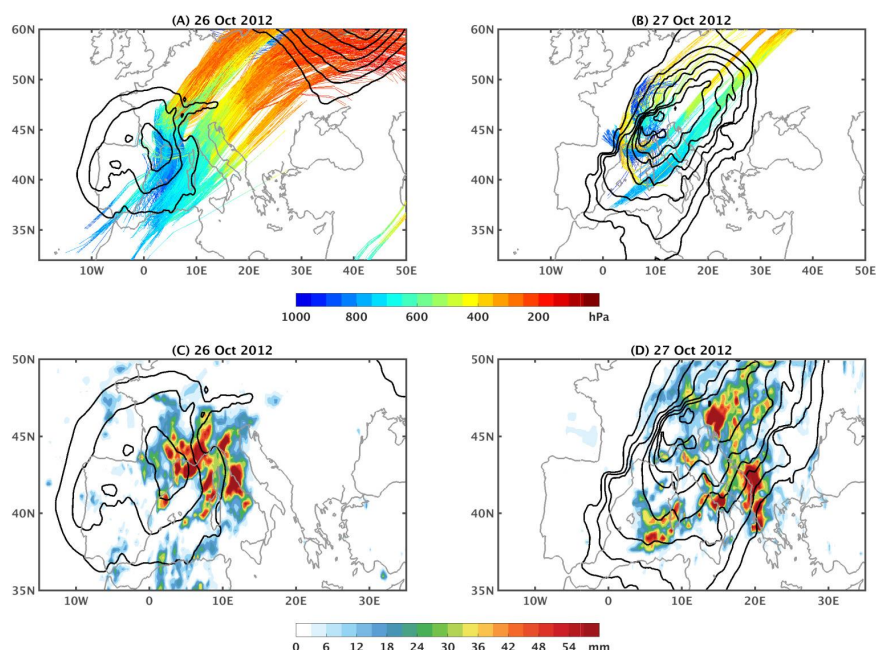


330 coexisted to attribute large amounts of rainfall over the western Mediterranean (Figure
331 2).

332 Several past studies showed that HP in the Mediterranean basin is intertwined with the
333 occurrence of cyclones. Scheffknecht et al. (2017) showed that cyclones are present for
334 all HPEs over the Corsica island when examining the climatology in the period 1985-
335 2015. Embedded deep convection and WCBs are responsible for the grand majority of
336 total regional precipitation and its extremes (Jansa et al., 2001; Hawcroft et al., 2012;
337 Pfahl et al., 2014; Galanaki et al., 2016; Raveh-Rubin and Wernli, 2015). As a token of
338 cyclones contribution to regional rainfall, Flaounas et al. (2018) showed that the 250
339 most intense systems of the period 2005-2015 were alone responsible for up to a third
340 of the total 11-year precipitation, while climate modelling showed that cyclones
341 contributed from 70% to almost the total of rainfall extremes, depending on the area
342 (Flaounas et al., 2015b). Such heavy rainfall events are related to water sources from
343 the Mediterranean Sea, but also from the tropical and extratropical Atlantic Ocean. This
344 is due to cyclogenesis being preceded by Rossby wave breaking over the Atlantic that
345 favours the eastward zonal transport of water vapour from oceanic remote areas,
346 rendering water vapour imports imperative for the formation of heavy rainfall in the
347 Mediterranean (Duffourg and Ducrocq, 2013; Flaounas et al., 2019).

348

349



350

351 **Figure 2:** (a) Sea level pressure (black contours every 3 hPa, outer contour is set at
 352 1005 hPa). Coloured lines show 48-hour air mass trajectories from ECMWF analyses
 353 that correspond to WCBs and where strong ascent takes place at 12:00 UTC, 26 Oct.
 354 2012 (i.e., when cloud ice occurs for the first time in the air masses). Vertical level of the
 355 air masses is shown in colour. (b) as in (a), but a strong ascent takes place at 12:00
 356 UTC, 27 Oct. 2012. (c) Daily accumulation of precipitation on 26 Oct. 2012 taken from
 357 3B42 of TRMM (colour). (d) as in (c) for 27 Oct. Datasets and methods are detailed in
 358 Flaounas et al. (2015a).

359

3.2 Advances in moist processes understanding

360

3.2.1 Distribution, origin, and transport of the water vapour supply to HPEs

361

362 The relevance of atmospheric water vapour distribution and stratification in the initiation,
 363 intensification, and maintenance of HPEs has been extensively demonstrated (e.g.,
 364 Duffourg et al., 2018; Lee et al., 2018), as well as the role of the Mediterranean Sea as
 365 a significant heat and moisture source for HPEs in the WMed area (Duffourg and
 366 Ducrocq, 2011; Flaounas et al., 2019). The scarcity of water vapour observations at the
 367 mesoscale and smaller scales, as well as the model limitations, for example in relation
 368 to the adequate spatial and temporal resolution and/or an accurate representation of the



vertical stratification, hampered progresses in the past. Indeed, our understanding of the variability of water vapour in relation to convection is still far from being complete. Large uncertainties remain regarding the origin, pathways, and timescales of transport of the large amounts of moisture necessary for HPEs in the WMed. The characterization and better understanding of the water vapour supply to HPEs has been a key aspect of the HyMeX field campaign and subsequent studies. The unprecedented deployment of instruments during the SOP1 for the monitoring of water vapour dynamics and the posterior cross-validation studies and synergetic use together with models allowed the many advances achieved in this period as described in the following.

One of the HyMeX observational highlights has been the dense network of GPS stations, over one thousand ground-based receivers, providing a reprocessed dataset specially produced for the HyMeX SOP (Bock et al., 2016). The large extent and high-density coverage of the reprocessed GPS network allowed a consistent representation of large-scale features, as well as smaller spatial and temporal scales in agreement with high-resolution simulations (Bock et al., 2016). Using the reprocessed integrated water vapour (IWV) GPS data Khodayar et al. (2018) showed that all HPEs within the north-western Mediterranean form in periods/areas characterized by IWV values in the order of 35-45 mm after an increase of 10-20 mm, being the most intense events those experiencing a more sudden increase (between 6 to 12 h prior to the event). Bock et al. (2016) demonstrated that regions prone to HPEs in autumn are characterized by high IWV variability up to 8 kg/m².

In addition to the unprecedented (in terms of spatial and temporal coverage) amount of information provided by the postprocessed GPS network, modelling studies are helpful for the assessment of potential sources of moisture. Recent advances in this topic showed that evaporation from the Mediterranean accounts for only about 40% (60%) of the water vapour feeding the deep convection developed over southeastern France when cyclonic (anticyclonic) conditions prevails in the days preceeding the event (Duffourg and Ducrocq, 2013). The Atlantic Ocean (Turato et al., 2004; Winschall et al., 2011; Duffourg et al., 2018; Flaounas et al., 2019) and tropical Africa (Krichak et al., 2015; Chazette et al., 2015b; Lee et al., 2016, 2017) have been also suggested as potential sources of moisture for HPE occurring in the western Mediterranean. The large-scale uplift of enriched African moisture plume and their role in gradual rain out of the air parcel over southern Italy during IOP13 were highlighted in a modelling study taking advantage of stable water isotopes by Lee et al. (2019). Backward trajectory analysis showed that the large-scale moisture transport takes place during about 3 to 4 days in the warm sector of front, whereas the surface evaporation over the Mediterranean occurs



405 shortly in a few hours to 1 day. Associated with extreme precipitation events over Italy,
406 whether convective or orographic, a recent study by Grazzini et al. (2019) confirmed the
407 systematic occurrence of anomalously high values of meridional Integrated Vapour
408 Transport that sometimes occurs in narrow filament shape regions of high integrated
409 moisture, called atmospheric rivers (Davolio et al., 2020), as during the 2011 Liguria
410 floods (Rebora et al., 2013) or the last extreme storm in October 2018 (Giovannini et al.,
411 2021) and October 2020 (Magnusson et al., 2021).

412 **3.2.2 Assessment of the variability and vertical distribution of the** 413 **atmospheric water vapour**

414 The variability and vertical distribution of the atmospheric water vapour and their
415 accurate representation in models have been demonstrated to play a key role for the
416 timing, location, and intensification of deep convection (e.g., Khodayar et al., 2018), thus
417 for the simulation of HPEs. They have been further identified as responsible for
418 inaccuracies in RCMs when compared against convection-permitting NWP models
419 (Khodayar et al., 2016a). To contribute to the characterization of the water vapour
420 variability, the ground-based WALI in the Balearic Islands, the airborne water-vapour
421 differential absorption lidar LEANDRE 2 on board the ATR42 aircraft, and boundary layer
422 pressurized balloons (BLPB; Doerenbecher et al., 2016) were deployed during the
423 SOP1. Water Vapour Mixing Ratio (WVMR) profiles were measured with a horizontal
424 resolution of 1 km (e.g., Flamant et al., 2015; Flaounas et al., 2015a; Chazette et al.,
425 2015a, 2015b; Di Girolamo et al., 2017; Duffourg et al., 2016; Lee et al., 2016, 2017). In
426 a multi-instrument and multi-model assessment of atmospheric moisture variability in the
427 north-western Mediterranean, Chazette et al. (2015b) demonstrated the consistency and
428 self-coherence of these water vapour data sets during the SOP1 pointing out the strong
429 need in assimilating high-resolution water-vapour profiles in the lowest layers as those
430 from lidar instruments. In a multi-scale observational investigation of atmospheric
431 moisture variability in relation to HPEs formation in the same region, Khodayar et al.
432 (2018), profited from the synergetic use of the observational datasets demonstrating that
433 the sampling of spatial inhomogeneities on different scales is crucial for the
434 understanding of the timing and location of deep convection. Furthermore, focusing on
435 the complex island of Corsica during SOP1, multiple observations from the mobile
436 observations platform KITcube (Kalthoff et al., 2013) further demonstrated the benefit of
437 integrated measurement systems (Adler et al., 2015).

438 The ground-based lidar WALI was useful in capturing the moist and deep boundary
439 layers with updrafts reaching up to 2 km in pre-convective environments leading to HPEs,



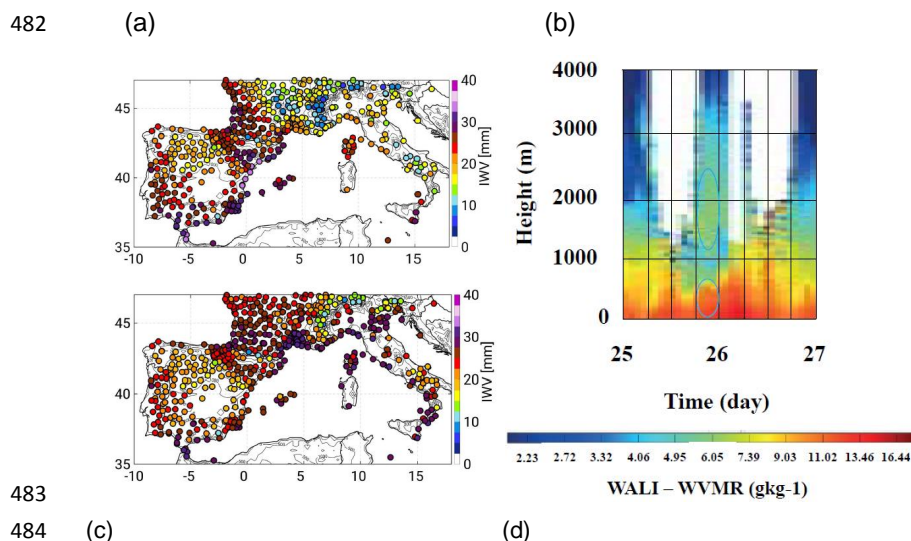
contrary to the dry, shallow boundary layers everywhere else (Khodayar et al., 2018). In Chazette et al. (2015a), the ground-based lidar WALI, additionally captured the increasing moistening of the free troposphere, up to 5 km, prior and in relation to the MCS formation. Furthermore, the specific humidity observations from BLPB and aircraft flights captured spatial inhomogeneities in the lower boundary layer up to 4 g/kg in less than 100 km, which were shown to determine the location of convection initiation (Khodayar et al. 2018).

Figure 3 illustrates for the IOP16 the complex moisture flow that fed the convective systems, which was effectively monitored by the variety of water vapour profiling sensors involved in combination with backward and forward trajectory analyses from a Lagrangian model (NOAA HYSPLIT Lagrangian trajectory model; Draxler and Hess, 1998; Rolph et al., 2017; Stein et al., 2015) and the information derived from the GPS network.

In Figure 3a, the spatial distribution of the 24 h-averaged GPS-derived IWP on 25 and 26 October 2012 shows initially higher atmospheric moisture content in the western area, where convection initiation takes place, whereas on the next period the humid air mass has advanced eastwards. The water vapor mixing ratio as measured by WALI in Ciutadella (Menorca) (Figure3b) reveals the presence of two distinct humid layers in the time interval 18:00–00:00 UTC on 25 October 2012: a surface layer extending up to about 0.6 km, with mixing ratio values up to $\sim 12 \text{ g kg}^{-1}$, and an elevated layer extending from 1.1 to 2.5 km, with mixing ratio values up to $6\text{--}7 \text{ g kg}^{-1}$. The 24 h forward trajectory analysis starting in Ciutadella at 21:00 UTC on 25 October 2012 at the altitudes of the observed humidity layers (Figure 3c) shows the northward movement of the surface humid layer, while air masses within the elevated humidity layer moved north-eastward. The latter are plausibly related to the inflow branch of WCBs, i.e., the blue part of the air mass trajectories in Figure 2. The surface humid layer overpassed Candillargues about 15–21 hours later, as proved by the mixing ratio profile measurements carried out by BASIL and illustrated in Figure 3e, possibly feeding the MCS forming close to the cyclone centre over the Cévennes-Vivarais region in the morning of 25 October. Indeed, the water vapour profile shown in Figure 3e is consistent with the one provided by LEANDRE 2, on board the ATR42 aircraft that flew over the WMed (Figure 12 in Flaounas et al., 2015a). The 24 h forward trajectory analysis also reveals that air masses within the elevated humid layer overpassed the Gulf of Lion, possibly ending up with feeding the offshore MCS system. Figure 3d additionally illustrates the 200-h back-trajectory analysis ending in Minorca at 21:00 UTC on 25 September 2012 at the altitudes (500 m



and 2000 m) where the two humid layers were observed, revealing that air masses within the surface humidity layer originated over the tropical Atlantic Ocean approximately 8 days earlier and overpassed Morocco and Southern Spain, slowly subsiding (in the last 72-96 hours before the formation of them MCS) upon reaching the Mediterranean basin from an altitude of 1000 m down to 500 m, whereas the air masses within the elevated humid layer originated over Central Africa (Northern Mali) approximately 3 days earlier and transited over Mauritania and Morocco before reaching the Balearic Islands.



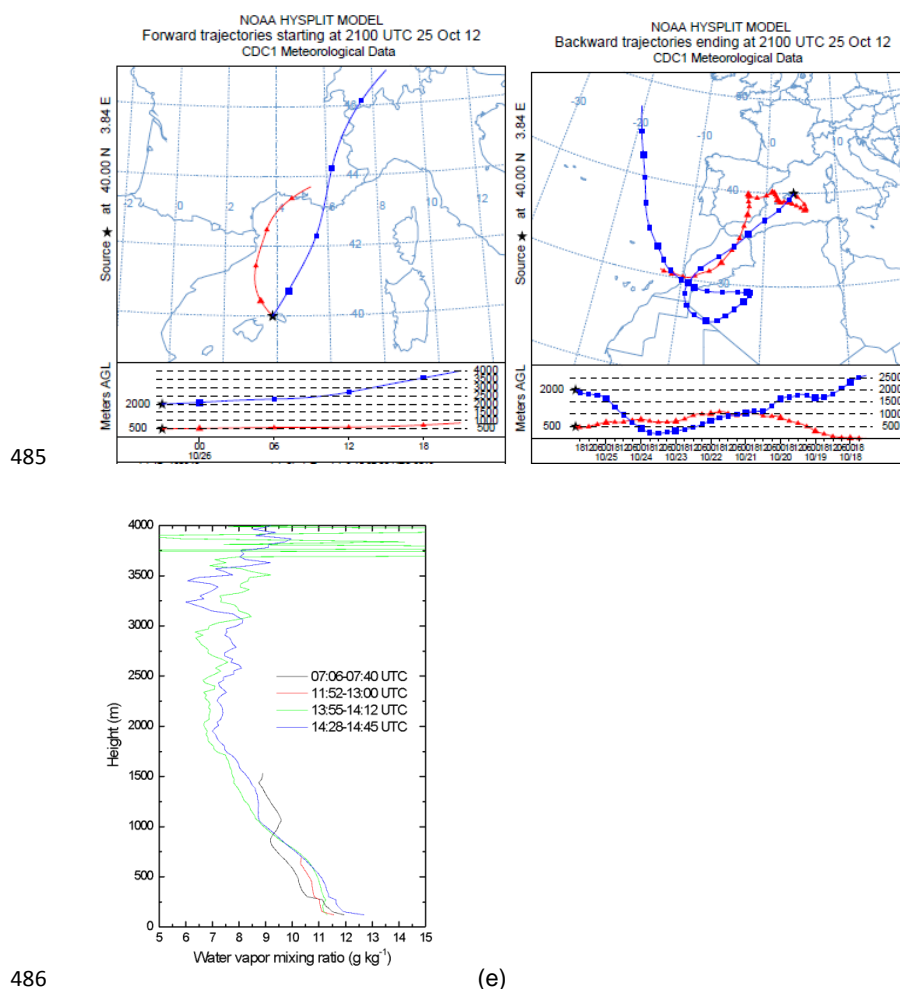


Figure 3: (a) Spatial distribution of 24 h-averaged GPS-derived IWV (mm) on 25 (top), and 26 (bottom) Oct. 2012. (b) Time evolution of the water vapor mixing ratio (g kg^{-1}) as measured by the ground-based lidar WALI in Menorca over the 48-h period from 00:00 UTC, 25 Oct. 2012 to 00:00 UTC, 27 Oct. 2012. (c) 24-h forward trajectory analysis from HYSPLIT starting in Ciutadella (Menorca) at 21:00 UTC, 25 Oct. 2012 and ending at 21:00 UTC, 26 Oct. 2012 and (d) 200-h back-trajectory analysis from HYSPLIT ending in Ciutadella (Menorca) at 21:00 UTC, 25 Oct. 2012. (e) Vertical profiles of the water vapor mixing ratio (g kg^{-1}) as measured by the ground-based lidar BASIL in Candillargues at different times on 26 Oct. 2012.

3.3 Low-level dynamical processes



497 Once the synoptic setting becomes favourable for heavy precipitation in the WMed , with
498 an upper-level trough slowly evolving eastward while deepening over the basin, the
499 mesoscale organization and the thermodynamic characteristics of the low-level flow
500 determines the occurrence, intensity and location of heavy precipitation. Most of the
501 severe rainfall events that occurred during the SOP1 field campaign can be connected
502 or at least interpreted in the framework of recent theoretical results concerning moist
503 orographic convection (Miglietta and Rotunno, 2014; Kirshbaum et al., 2018). However,
504 their in-deep analysis has revealed a greater complexity of real meteorological situations,
505 due to non-stationarity, to the complexity of the real 3D orography and vertical profiles,
506 and especially to the interaction among small-scale processes, which are not entirely
507 accounted for in controlled-environment numerical experiments. One of the merits of
508 HyMeX has been to provide evidence of the theoretical results and to enrich our
509 knowledge on genesis and evolution of convection in a complex topography environment
510 through a plethora of modelling simulations and tools, and advanced instrument
511 observations.

512 Being heavy orographic precipitation in stable and neutral atmospheric conditions
513 already investigated in past experiments (e.g., MAP-Mesoscale Alpine Programme,
514 Bougeault et al., 2001) and well understood, the focus of HyMeX was on the
515 development of quasi-stationary MCSs, well known responsible of recent HPE and floods
516 in the area (Nuissier et al., 2008; Buzzi et al., 2014; Romero et al., 2014 among others).
517 These systems are characterized by “back-building” processes that force the continuous
518 redevelopment of deep convective cells over the same area producing severe and
519 persistent rainfall (Schumacher and Johnson, 2005; Ducrocq et al., 2008; Duffourg et al.,
520 2018; Lee et al., 2018). The multicell MCSs resulting from this retrograde regeneration
521 assume a typical V-shaped pattern in radar and satellite images. In this context,
522 conditionally unstable marine flow directed towards the coastal mountainous regions and
523 extracting energy from the sea surface has been pointed out as a common feature of all
524 the events. However, different convection-triggering mechanisms have been identified
525 and highlighted.

526 **3.3.1 Convection-triggering mechanisms**

527 Low-level convergence over the sea can initiate convection even far from the coast and
528 usually it is produced by the large scale forcing. During IOP16 (Duffourg et al., 2016) the
529 cyclonic circulation around a shallow low-pressure system was responsible for low-level
530 convergence against the south-easterly flow, between Balearic Island and the Gulf of
531 Lion (Figure 4a). Lee et al. (2016) revealed the key role during IOP13 of an approaching



532 cold front in modifying the low-level circulation over the Tyrrhenian Sea, establishing
533 favourable dynamical conditions for convection initiation. Even for the IOP8, the low-level
534 convergence that first triggered convection south of the Iberian Peninsula was ascribed
535 to the large-scale setting (Röhner et al., 2016; Khodayar et al., 2015), even if orographic
536 effects were essential to enhance mesoscale uplift over land during the mature phase of
537 the convective system.

538 In fact, due to the peculiar topographic characteristics of the basin, in most of the events
539 it is the interaction with the orography that triggers and eventually maintains convection,
540 since it does provoke not only the direct lifting, but can also produce the convergence
541 required to initiate vertical motions. Several numerical experiments (Barthlott and
542 Davolio, 2016) clearly showed the effects of Corsica and Sardinia on the downstream
543 low-level wind as well as on temperature and moisture distribution. In particular, the
544 deflection of the westerly/south-westerly flow due to the complex orography of the islands
545 was identified as a key mechanism for the organization of heavy precipitation along the
546 western Italian coast, since it determined small-scale complex patterns of low-level
547 convergence over the sea in the lee of Corsica, where convection was triggered (Figure
548 4b). Moreover, the interaction between sea breezes and drainage winds induced by
549 mountainous islands like Corsica or Sardinia (Barthlott and Kirshbaum, 2013; Barthlott
550 et al., 2016) impacts on the development of deep convection both offshore and anchored
551 to topographic features. Also, the flow splitting around Corsica Island can be a key
552 mechanism producing a lee-side convergence line where a severe and stationary
553 convective system develops (Scheffknecht et al., 2016).

554 Interestingly, the study of Lee et al. (2017) clearly indicated that neither an offshore
555 convergence line nor the orographic uplift alone would have been enough to allow the
556 development of the intense MCS that affected the Ebro River valley during IOP 15
557 (Figure 4c). It was their interplay that produced deep convection, together with the
558 simultaneous presence of flow channelled by the local orography and converging with
559 the low-level marine inflow. This represents a clear example of the complex interaction
560 among processes that HyMeX was able to highlight.

561 Low-level convergence induced by blocking effect of mountain chains on the impinging
562 flow is another frequent lifting mechanism upstream of the orography. Well before the
563 HyMeX SOP, it was demonstrated that flow blocking in front of Massif Central and the
564 enhanced convergence due to deviation of southerly flow around the Alps (Figure 4d)
565 (Ducrocq et al., 2008; Davolio et al., 2009), were responsible for several HPE over
566 southeastern France, affecting areas well upstream of the main orographic reliefs. SOP



related studies identified a similar low-level flow characteristic, associated with heavy rainfall over north eastern Italy. In both the analysed events, occurred during IOP2b (Manzato et al., 2015; Miglietta et al., 2016) and IOP 18 (Davolio et al., 2016), the blocking of southerly low-level marine inflow in the form of a north-easterly barrier wind in front of the Alps, produced strong and localized convergence, favouring convection triggering (Figure 4e). Through additional modelling investigation of similar events in the past, this was recognised as a typical mechanism for deep convection (even supercell) development over the area.

The importance of orographic interaction has been revealed also for the development of lee-side convection. Pichelli et al. (2017) through a number of numerical simulations of IOP6 illustrated the complex and delicate equilibrium between competing processes (orographically induced subsidence on the lee side and frontal uplift) that determined the evolution of a squall line over the Po Valley, in the lee side of a mountain range (Apennines) with respect of the main southerly flow feeding the precipitation.

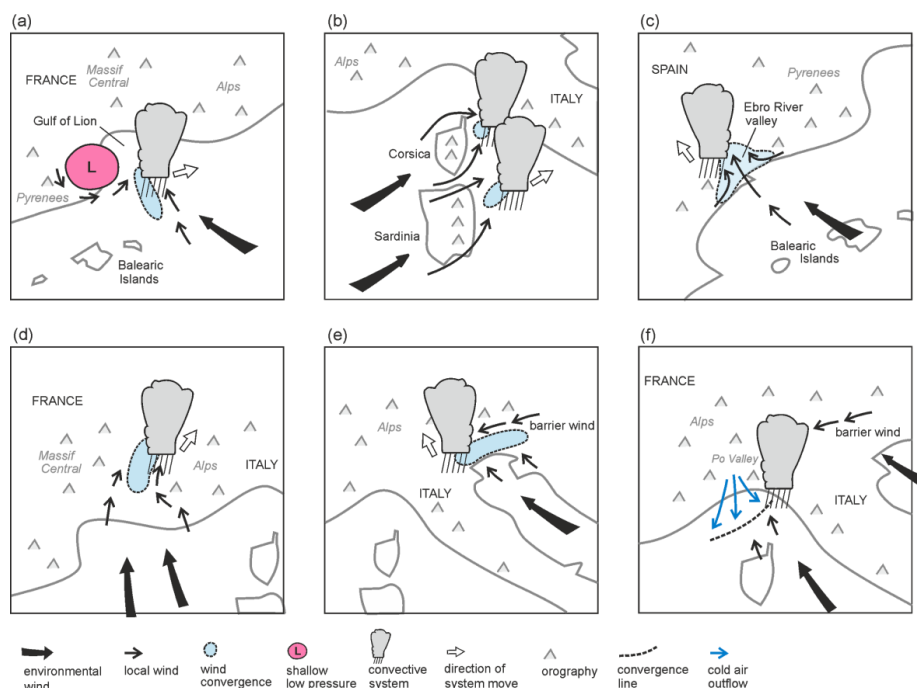


Figure 4: Conceptual illustrations of key convection-triggering mechanisms in the north-western Mediterranean basin. Coast lines are depicted by grey solid lines.



585

3.3.2 Cold pools

586 The detailed observational and modelling analysis of IOP13 revealed that, as expected,
587 also the direct orographic uplift can trigger convection close to the coastal slopes.
588 However, thanks to detailed observations and modelling simulations of the precipitation
589 system and of the upstream environment, Duffourg et al. (2018) were able to provide a
590 thorough description of the mechanisms that maintained the MCS while slowly moving
591 offshore. In fact, the formation of an evaporative cold pool under the precipitating cells
592 generated down-valley flows that slowly shifted the location of the back building
593 convective cells from the mountain to the coast and over the sea.

594 In this regard, it was emphasized (Lee et al., 2018) that the moisture vertical distribution
595 in the lower troposphere can modulate the intensity of the cold pool and thus to control
596 location and amount of heavy precipitation associated with the MCS. In several other
597 events, the leading edge of a cold pool, formed by evaporative cooling under the
598 precipitating cells, was able to trigger convection by lifting the impinging ambient low-
599 level flow. As suggested by idealized experiments of conditionally unstable flow over a
600 mountain ridge (Bresson et al., 2012; Miglietta and Rotunno, 2009), the stationarity of
601 the MCS or its upstream propagation away from the orographic barrier is determined by
602 the intensity of the ambient flow. In this context, the vertical structure of the lower
603 troposphere, in terms of moisture content and wind intensity, represents an important
604 factor since it modulates the evaporation potential and thus the formation and intensity
605 of the cold pool.

606 However, the presence of cold and dense air acting as a virtual mountain with respect to
607 the impinging warm and moist flow can be due to different processes besides
608 evaporative cooling. In the analysis of IOP8, Bouin et al. (2017) identified cold and moist
609 air masses transported from the Gulf of Lion by the low-level jet. Despite their moisture
610 content, these air masses were cold and dense enough so that their accumulation on
611 the foothills of the relief contributed to initiating a cold pool. Once the MCS was triggered,
612 rain evaporation in the subsaturated mid-level layer resulted in downdraughts that further
613 intensified the cold pool, favouring the regeneration of the precipitation system. Finally,
614 investigation of heavy precipitation over Liguria in IOP16 as well as in previous dramatic
615 HPE, undertaken within the HyMeX framework, provided a clear picture of the
616 mechanisms responsible for recent and recurrent disastrous floods along the Ligurian
617 Sea coast. Several studies (Buzzi et al., 2014; Fiori et al., 2017 among others) pinpointed
618 the role of the cold air outflow from the Po Valley, across the Apennine gaps, which
619 propagate as a density current to the Ligurian Sea, where it determined a sharp



mesoscale convergence line (sketched in Figure 4f). Along such a convergence line, the lifting of southerly moisture laden flow produced the onset of the severe convection. Interestingly, the cold flow over the sea appeared to be induced by an easterly inflow into the Po Valley from the Adriatic side, possibly due to a barrier wind effects over north-eastern Alps as previously described. As observed in many other cases (e.g., Duffourg et al., 2016) although the V-shape structure seems anchored over the sea, a few tens of kilometres offshore, intense convective cells are continuously advected inland where HP occurs. Finally, Duffourg et al. (2016) also highlighted an interesting feedback process of convection to the environment that, through small-scale perturbations of the low-level circulation around the cold pool, focussed and reinforced the local moisture convergence feeding the convective updraft.

3.4 Impacts of the land and the sea surfaces

3.4.1 Land conditions and feedback to the atmosphere

Land conditions and feedbacks between the land surface and the atmosphere play a role in determining the response of the Earth system to climate change, particularly in the Mediterranean region, which is a transitional zone between dry and wet climates. Indeed, enhanced land–atmosphere feedbacks are expected in a warming climate, and their understanding and simulation are challenging, but fundamental to further improve our knowledge about future climate and their interactions with the other components of the climate system. Despite its relevance, the modelling of land-atmosphere feedbacks still suffers for relevant uncertainty owing to inaccurate initialization, and/or model physics, misspecified parameters, etc... Helgert and Khodayar (2020) showed that an improvement of the soil-atmosphere interactions and subsequent HP modelling is observed using an enhanced initialization with remote sensed 1 km SM information. Khodayar and Helgert (2021) additionally investigated the response of the western Mediterranean HP to extreme SM conditions showing that changes in the initial scenarios impact the mean, but also the extremes of precipitation. Regional projections of precipitation under the RCP4.5 and RCP8.5 scenario have shown to be considerably modified when SM is used as predictor (Hertig et al., 2018). Therefore, a better knowledge and representation of soil conditions and evolution have to be considered for HP understanding and modelling.

3.4.2 Air-sea interactions and coupling

The Mediterranean Sea and the atmospheric boundary layer (ABL) continuously exchange momentum, heat, and freshwater. These exchanges, related to the turbulent fluxes, are controlled by the gradients of temperature, humidity, and velocity at the air-sea interface. Rainaud et al. (2015) showed that although moderate air-sea fluxes were



656 observed during the HPEs of SOP1, large air-sea exchanges in the Gulf of Lion and the
657 Balearic, Ligurian and Tyrrhenian Seas can be correlated to the occurrence of a HPE.
658 The SST strongly influences the low-level flow stability and dynamics through heating,
659 moistening and downward momentum mixing (Stocchi and Davolio, 2017; Meroni et al.,
660 2018a). SST is indeed a key parameter for evaporation (Figure 5a) and its influence on
661 HPEs in terms of convection triggering, intensity, and location, has been extensively
662 investigated with several numerical studies (e.g., Strajnar et al., 2019; Senatore et al.,
663 2020b, for some of the most recent). Generally, these studies highlight that the SST
664 values strongly and directly modify the low-level atmospheric stability, which first impact
665 the intensity of convection and precipitation, with the most intense rainfall associated
666 with warmer sea surface. The location and stationarity of heavy precipitating systems
667 are also modified, with an acceleration of the low-level wind velocity over warmer sea,
668 but also by the fine-scale SST horizontal patterns with eddies and marked fronts in the
669 Mediterranean (as explicitly simulated in the coupled forecast of Rainaud et al. (2017)
670 for IOP16a shown in Figure 5a) that can significantly change the flow dynamics
671 interacting with orography (Davolio et al., 2017) or displace the moisture convergence at
672 sea (Rainaud et al., 2017; Meroni et al., 2018a).

673 During intense meteorological events in the Mediterranean such as HPEs, significant
674 modifications of the ocean mixed layer (OML) can occur, even on short timescales of
675 only several hours (Lebeaupin Brossier et al., 2014), and can significantly impact the
676 exchanges with the ABL. Berthou et al. (2016) showed that IOP16a was likely sensitive
677 to SST changes upstream related to OML changes and sub-monthly air-sea coupling.
678 The ocean vertical stratification is also a characteristic which has to be accounted for, as
679 sea surface cooling during HPEs is largely controlled by the entrainment of deeper and
680 colder water in the OML. The study of Meroni et al. (2018b) using coupled experiments
681 with idealized ocean conditions highlights that the cooling is more pronounced with a
682 shallow, strongly stratified OML, leading to lower air-sea fluxes, less air instability and
683 finally a reduction of the total amount of simulated precipitation.

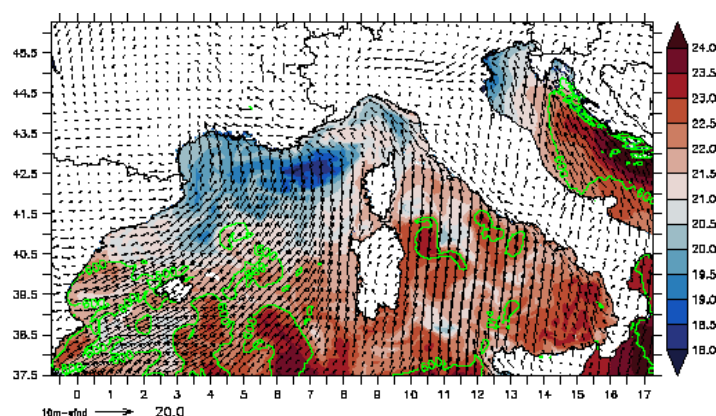
684 The use of ocean-atmosphere coupled systems enables us to consider the ocean 3D
685 structure and its interactive and consistent evolution. Such modeling systems were
686 specifically developed in the framework of HyMeX to improve the realism of weather
687 forecasts for sea surface and atmospheric low levels, and innovatively evaluated thanks
688 to the multi-compartments' observational dataset. For IOP16a, Rainaud et al. (2017)
689 showed that, due to mixing and heat loss, the progressively lower SST in the coupled
690 model induces lower heat fluxes (-10% to -20% of evaporation), local differences in the



691 low-level environment (stability) and cyclonic circulation, with small impacts on the
 692 convection organization (convergence) and intensity.

693 Waves also impact the atmospheric low levels, by increasing the surface roughness and
 694 the momentum flux and act as a drag for the low-level upstream flow. For HPEs, in forced
 695 and coupled simulations, this slow-down results in modification of HP location due for
 696 instance to changes in the low-level flow, convergence line or cold pool motion over the
 697 sea (Bouin et al., 2017; Sauvage et al., 2020). The study of Thévenot et al. (2015)
 698 highlighted this waves impact in the IOP16a case, with a better representation of the low-
 699 level moist jet feeding the MCSs and of the simulated precipitation when sea state is
 700 considered in the bulk formulae (Figure 5b).

(a)



(b)

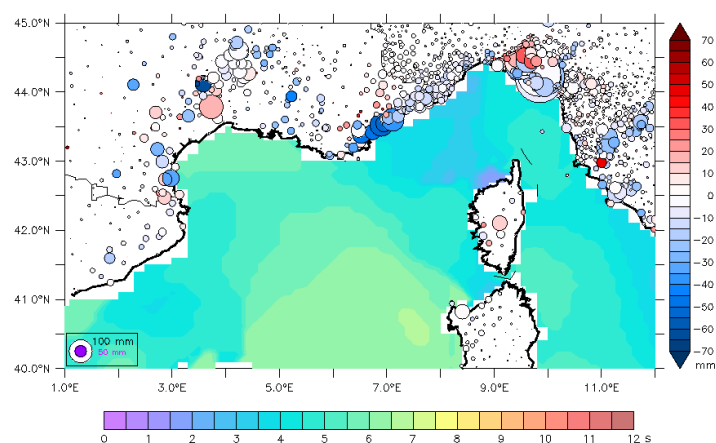




Figure 5: (a) Daily mean SST (colours, °C), 10m-wind (arrows, m s^{-1}) and surface evaporation (green contours for values above 600 kg m^{-2}) for 26 Oct. 2012 (IOP16a) from the AROME-NEMO WMED coupled experiment (CPLOA) of Rainaud et al. (2017). (b) Peak period of waves (color, s) at 00:00 UTC, 26 Oct. 2012 considering in Thévenot et al. (2016) and bias modification (circles, mm) for 24h-rainfall accumulation against rain-gauges data, comparing MESO-NH simulations with (WAM) and without (NOWAV) sea state impact (blue for an improvement in WAM). The size of the circles indicates the NOWAV bias (absolute value, in mm).

701

702

703 3.5 Microphysics

704 Many advances in the understanding and knowledge of cloud composition and
 705 microphysical processes in Mediterranean convective systems were attained in the
 706 framework of HyMeX, thanks to the large number of observations used in process,
 707 modeling and/or data assimilation studies.

708 Among them, a large number of available disdrometers and MRRs were used to improve
 709 the quality of observations (Raupach and Berne, 2016 and Adirosi et al., 2016) and the
 710 characterization of the raindrop's PSD (Adirosi et al., 2014, Adirosi et al., 2015, Schleiss
 711 and Smith, 2015), including its very small-scale variability (Gires et al., 2015).

712 Based on rain gauge observations over a long period encompassing the HyMeX
 713 experiment, Molinié et al. (2012) studied the rainfall regime in a mountainous
 714 Mediterranean region, in southeastern France. They found that rainfall intermittency,
 715 both at the monthly and daily scales, is well correlated to the rain gauge altitude, which
 716 is also linked to rainfall intensity. Zwiebel et al. (2015) and Hachani et al. (2017) also
 717 found that several factors (altitude, season, weather type, among others) influence both
 718 the rainfall characteristics at the ground and the relationship between rainfall rate and
 719 the reflectivity factor.

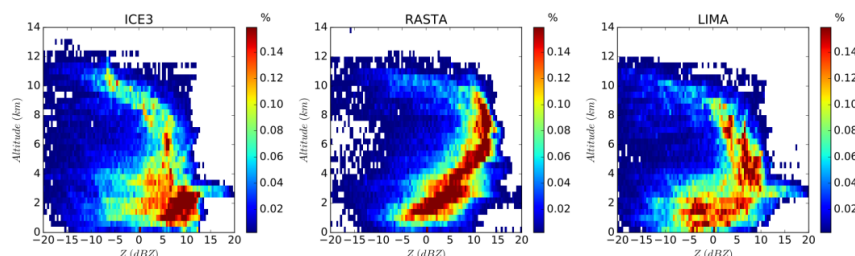
720 Other studies focused on the use of radar data to investigate the cloud composition.
 721 Grazioli et al. (2015) proposed a hydrometeor classification algorithm using an X-Band
 722 radar (deployed in Ardèche during HyMeX SOP1). Ribaud et al. (2015) also developed
 723 a hydrometeor classification algorithm using dual-polarimetric radars and produced 3D
 724 hydrometeor fields when several radars were available. Using this classification, they
 725 also identified a link between cloud characteristics and lightning propagation (Ribaud et
 726 al., 2016).

727 HyMeX microphysical observations have also led to improvements in model physics and
 728 parameterizations. Fresnay et al. (2012) first demonstrated the sensitivity of



729 Mediterranean HPEs simulations to the cloud parameterization. Using several
 730 observations from HyMeX SOP1, Taufour et al. (2018) showed that the 2-moment
 731 scheme LIMA (Vié et al., 2016) provides a more realistic cloud representation than the
 732 1-moment scheme ICE3. This is shown in Figure 6 comparing observed and simulated
 733 RASTA reflectivities. The shape of the reflectivity distribution is better represented by
 734 LIMA than ICE3, especially in the melting region. Furthermore, they proposed a revision
 735 of the scheme LIMA based on the disdrometer rain PSD observations.
 736 The aerosol-cloud interactions were also found to have a strong impact on convective
 737 systems and rainfall characteristics (Kagkara et al., 2020), and the best simulation results
 738 with the 2-moment scheme LIMA are obtained when using a realistic aerosol population
 739 from the MACC analyses validated against ATR42 observations (Taufour et al., 2018).
 740 Eventually, some studies prepared the future assimilation of cloud data. Augros (2015)
 741 implemented the assimilation of dual-polarization radar data in the French operational
 742 AROME model. Borderies et al. (2019a, 2019b) proposed a method to assimilate
 743 airborne RASTA reflectivities and Doppler winds, meanwhile releasing an improved
 744 version of the RASTA simulator for use in mesoscale models.

745



746

747 **Figure 6:** Comparison of observed and simulated RASTA reflectivities, merging data
 748 from IOPs 6 and 16a (From Taufour et al. 2016).

749

750 4. Improving Heavy precipitation modelling across scales

751 4.1 Increasing model resolution simulations

752 Idealized simulations of deep moist convection at kilometric scales (grid spacing: 4 km,
 753 2 km, 1 km and 500 m) showed that the accumulated rainfall and corresponding surface
 754 area, as well as the area covered by the updrafts, increase with increasing resolution. At
 755 4 km horizontal resolution, deep convection is under-resolved, and differences are larger
 756 between 1 km and 500 m horizontal resolution simulations than between 2 and 1 km,



757 suggesting the beginning of convergence at 500 m (Verrelle et al., 2014). Bassi (2014)
758 analysed several IOPs over LT target area performing numerical simulations at different
759 grid-spacings between 3 and 1 km, and with different resolutions of the orography
760 representation, showing that both aspects equally contributed to improve the quantitative
761 precipitation forecast (QPF). In fact, the higher model resolution allowed a better
762 description of the structure, vertical motions, and dynamical mechanisms of the
763 convective system, whereas accurate orography was required to correctly simulate the
764 propagation of the density current along the Apennine slopes, and thus the precise
765 location of the convergence line that triggered the MCS. In terms of microphysics
766 parameters, discrepancies between models and observations could be attributed to the
767 implementation of one-moment microphysics scheme and to the coarse resolutions,
768 hence, there is a need for grid spacing finer than 2.5 km (Augros et al., 2015).

769 The increase in horizontal resolution is therefore a great improvement but it additionally
770 poses challenges for the model physics since some parameterization schemes may
771 become inappropriate. This is the case, for example, of the turbulence parameterization
772 in the “grey zone” between 1 km and 100 m horizontal grid spacing (Wyngaard and Coté,
773 1971), or of one-moment microphysical schemes where the overestimation of
774 reflectivities at high altitude due to graupel is a known limitation (Varble et al., 2011).

775 Hectometric-scale simulations of a Mediterranean HP event at 150 m by Nuissier et al.
776 (2020) were able to capture features regarding convective organization within the
777 converging low-level flow, which are out of range of models with kilometric horizontal
778 resolutions. However, the comparison of the large-eddy simulation (LES) with a
779 reference simulation performed with a 450 m grid spacing in the heart of the so-called
780 “grey zone” of turbulence modelling shows that the increase in resolution does not
781 significantly reduce deficiencies of the simulation, being this fact more related to an issue
782 of initial and lateral boundary conditions.

783 **4.2 New generation of high-resolution convection permitting simulations** 784 **and improvement of RCMs**

785 One of the most remarkable advances in the last years with significant implications for
786 HP simulation has been the development of the new generation of high-resolution
787 convection-permitting models (CPMs). This development has been extensively fostered
788 and exploited in HyMeX related activities and studies and represented one of the main
789 innovations contributing to advance knowledge in HP occurrence. Kilometric grid spacing
790 has become achievable with the increasing availability of computational resources. As
791 the horizontal resolution approaches 1 km, parameterization of deep convection is no



792 longer needed since much of the convective motion is explicitly resolved. It has been
793 demonstrated that the reduction of the grid spacing leads to a weaker overestimation in
794 height and size of the convective cells (Caine et al., 2013), together with a more accurate
795 representation of the timing and location of convection (Clark et al., 2016).

796 The benefit of higher horizontal resolution of CPMs can also propagate along the
797 forecasting chain to hydrological predictions. Simulating the catastrophic Liguria floods
798 of 2011, Davolio et al. (2015) demonstrated that the finer grid resolution resulted in better
799 QPF because of a more accurate description of the MCS and of its interaction with the
800 orography, and this improvement was confirmed also in terms of discharge forecasts.

801 In a seamless weather-climate multi-model intercomparison, Khodayar et al. (2016a)
802 showed that despite differences in their representation of a HPE, CPMs represented
803 more accurately the short-intense convective events, whereas the convection-
804 parameterized models produce a large number of weak and long-lasting events and
805 RCMs produce notably lower precipitation amounts and hourly intensities. Figure 7
806 shows an example of how finer resolution simulations better represent convergence over
807 the sea, where warm and moist air is transported by a low-level jet towards the French
808 coast. The higher resolution enhances the humidity convergence areas over the sea,
809 which appear located further upstream, as well as the associated triggering of
810 convection. Furthermore, the added value of convection-permitting with respect to RCMs
811 has also been demonstrated in the north-western Mediterranean basin (e.g., Berthou et
812 al., 2018; Coppola et al., 2018; Fumière et al., 2019). Berthou et al. (2018) showed that
813 convection permitting RCM simulations (about 2.5 km grid spacing) better represented
814 HPE in southern France in terms of daily precipitation than their convection-
815 parameterized counterparts (about 12.5 km grid spacing). It was also shown the added
816 value for the simulation of hourly rainfall over the United Kingdom, Switzerland, and
817 Germany. Coppola et al. (2018), in a multi-model study, proved the ability of high-
818 resolution CP-RCMs to reproduce three events of HP, one in summer over Austria, one
819 in fall associated with a major Foehn event over the Swiss Alps and another intense fall
820 event along the Mediterranean coast. In a dedicated study of Mediterranean HPEs in fall
821 on an hourly time scale, Fumiere et al. (2019) demonstrated that high resolution allows,
822 (a) the improved representation of the spatial pattern of fall precipitation climatology, (b)
823 the improvement of the localization and intensity of extreme rainfall on a daily and hourly
824 time scales, and (c) the ability to simulate intense rainfall on lowlands.

825

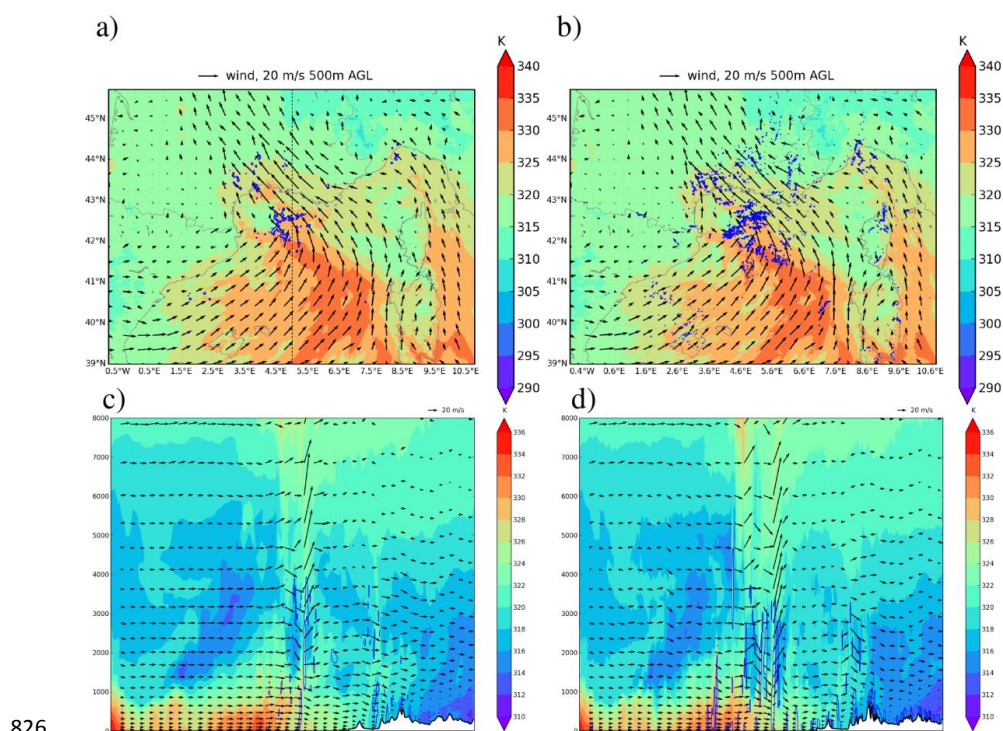


Figure 7: IOP16: 0930 UTC, 26 Oct. 2012. Horizontal cross sections at 500m AGL and vertical cross sections along a South-North line (shown in a) of equivalent potential temperature (K, in colour scale), and wind vectors (m s^{-1} , black arrows) for 2-km (left panels) and 500-m (right panels) resolution runs. The blue lines represent the humidity convergence ($-0.1 \text{ kg s}^{-1} \text{ m}^{-3}$ for vertical cross sections, and $-0.02 \text{ kg s}^{-1} \text{ m}^{-2}$ integrated value over the layer between the ground and 3000 meters for horizontal cross sections).

4.2 Improvement of parameterization schemes

Recent studies have shown that the simulation of convective systems is very sensitive to model parameterizations. For the IOP16a, Thévenot et al. (2015) showed that taking sea state into account in the turbulent air-sea exchanges can modify the low-level dynamics of the atmosphere and the precipitation location. However, the relationship of Oost et al. (2002) used in this study to compute the roughness length is known to overestimate the turbulent fluxes in strong wind regimes. New formulation of sea surface turbulent fluxes parameterization is under development and currently tested to better represent the wind-sea (i.e., the younger waves locally generated by wind) impact and related variability. The preliminary results when applied to HPE forecasts confirm the



844 significant slow-down of the upstream low-level flow with displacement of convergence
845 over the sea and show minor changes in the heat and moisture fluxes (Sauvage et al.,
846 2020). Further developments are planned concerning sea surface fluxes computation,
847 including notably the impact of sea spray on moisture and of the swell (i.e., the oldest
848 non-local waves).

849 In Rainaud et al. (2015), a change in the SST or the coupling of atmospheric and oceanic
850 models is found to have a large impact on the simulated precipitation amount over land.
851 Martinet et al. (2017) investigated the sensitivity of simulated HP at a sub-kilometric scale
852 (500 m) to the turbulence parameterization (i.e., Deardorff or Bougeault-Lacarrère)
853 showing that the simulated environment and convective processes are highly sensitive
854 to the formulation of the mixing-length. Convective systems are more intense in
855 association to larger moisture advection, higher hydrometeor contents and marked low-
856 level cold pools with weaker mixing lengths, since in this case the subgrid TKE is weaker,
857 and winds are increased to balance this effect.

858 Moreover, Verrelle et al. (2014) found insufficient turbulent mixing inside convective
859 clouds, more pronounced at kilometer resolution with weak thermal production,
860 underlying a lack of entrainment in convective clouds at intermediate range (between
861 500 m and 2 km horizontal resolution). By using LES of deep convection, Verrelle et al.
862 (2017) and Strauss et al. (2019) showed that the commonly used eddy-diffusivity
863 turbulence scheme (K-gradient formulation) underestimated the thermal production of
864 subgrid TKE and did not enable the nonlocal turbulence due to counter-gradient
865 structures to be reproduced. These two studies also found that the approach proposed
866 by Moeng (2010), parameterizing the subgrid vertical thermodynamical fluxes in terms
867 of horizontal gradients of resolved variables (H-gradient approach), reproduced these
868 characteristics, and limited the overestimation of vertical velocity. This new approach has
869 also been assessed using Meso-NH simulations at kilometer-scale resolutions for real
870 cases of deep convection on two HyMeX IOPs (IOP6 and IOP16a) (Ricard et al., 2021).
871 The new scheme enhances the subgrid thermal production of turbulence with a better
872 representation of counter-gradient areas and reduces the vertical velocity inside the
873 clouds (Figure 8). The enhanced turbulent mixing modifies the entrainment and
874 detrainment rates and produces more developed anvils with increased values of ice and
875 snow, which are more realistic. It also affects the cold pool under the convective cells.

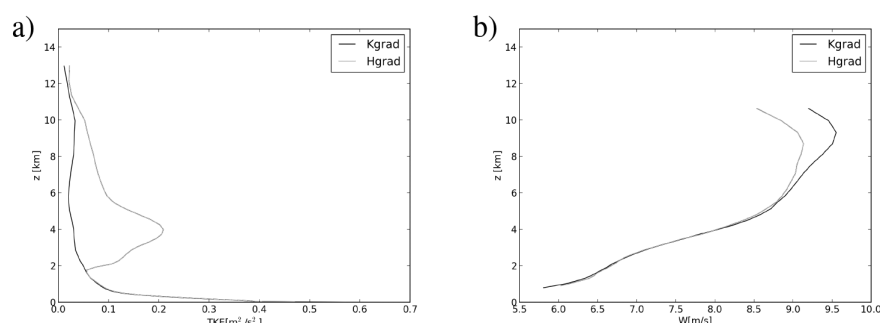


Figure 8: Mean vertical profiles inside the clouds of (a) subgrid TKE ($\text{m}^2 \text{s}^{-2}$) and (b) vertical velocity (m s^{-1}) during IOP16 (between 00:00 UTC, 26 Oct and 00:00 UTC, 27 Oct. 2012) for 2-km horizontal resolution Meso-NH simulations using K-gradient formulation (black line) and H-gradient formulation (grey line) for the vertical turbulent fluxes of heat and moisture.

4.3 Data Assimilation

One of the HyMeX goals was to improve or develop research- as well as operational-oriented atmospheric data assimilation systems and methods. Emphasis has been put on progresses in the processing of observations currently available in data assimilation systems and on the assimilation of new observation types, especially aimed at improving the prediction of HP.

A real-time implementation of the HyMeX-dedicated version of the Météo-France AROME NWP system covering the whole WMed ran from 01 September 2012 to 15 March 2013 (Fourrié et al., 2015). The same system was used to perform an extensive reanalysis of SOP1 exploiting observations from research instruments deployed during the campaign in addition to the operational observations assimilated in real-time (Fourrié et al., 2019). For that, processing of observations and systematic comparisons between observations and AROME short-range forecasts were carried out for: i) ground-based Lidar water vapour observations in Candillargues (BASIL) and at Menorca (WALI), ii) airborne Lidar LEANDRE II water vapour observations along the SAFIRE/ATR42 flight tracks, iii) high-resolution radiosoundings from operational sites in France and Spain and HyMeX -dedicated radiosoundings launched during SOP1 over France and Italy, iv) dropsondes observations and in-situ observations from the three research aircrafts, v) reprocessed wind profiler observations, vi) reprocessed delays from more than 1000 GPS receivers over France, Spain, Portugal and Italy, vi) radar data from five AEMET



903 operational radars over Spain, vii) additional SST observations from ship and Argo
904 floats. The skill scores showed a better performance for the forecasts starting from the
905 re-analysis than those starting from the real-time AROME-WMED analysis. Data denial
906 experiments, for which one of the above-listed datasets was removed from the reanalysis
907 at a time, clearly showed the benefit of assimilating the reprocessed GPS ground-based
908 zenithal total delays as shown in Figure 9.

909 This result was confirmed in other studies. Lindskog et al. (2017) demonstrated the
910 benefits of GPS assimilation to the forecast quality. Bastin et al. (2019) pointed out that
911 the general overestimation of low values of IWV in RCM models over Europe was
912 reduced when using a nudging technique to assimilate IWV information. Caldas-Alvarez
913 and Khodayar (2020) highlighted the positive impact exerted by moisture corrections on
914 precipitating convection and the chain of processes leading to it across scales.
915 Furthermore, the implementation of nudging methodologies to exploit non-conventional
916 observations, such as rainfall estimates from remote sensing, provided positive results
917 in applications to both nowcasting and short-term meteo-hydrological forecasting
918 (Davolio et al., 2017; Poletti et al., 2019).

919 The potential of several new types of observations within cloudy and precipitating
920 systems have been also investigated. As a first step towards assimilation, “observation
921 operators”, which consist in simulating observations from model outputs, have been
922 developed. In the framework of HyMeX, a dual-polarization weather radar simulator has
923 been developed in the post-processing part of the Meso-NH mesoscale model (Augros
924 et al., 2015). An observation operator for the airborne Rasta reflectivity observations has
925 also been developed (Borderies et al., 2019a). The impact of the assimilation of RASTA
926 data on AROME-WMED analyses and forecasts has been assessed. IOP7a results
927 indicated an improvement in the predicted wind at short-term ranges (2 and 3 hours) and
928 in the 12-hour precipitation forecasts. Over a longer cycled period, a slightly positive
929 improvement in the 6-, 9- and 12-hour precipitation forecasts of heavy rainfall has been
930 demonstrated (Borderies et al., 2019a). The assimilation of RASTA reflectivity data in
931 AROME-WMED over the whole SOP1 period resulted in an improvement of rainfall
932 forecasts even larger when wind was jointly assimilated (Borderies et al., 2019b).

933 Finally, HyMeX has fostered the inception of a collaboration between CNRM (France)
934 and CNR-ISAC (Italy) concerning the assimilation of radar data. The assimilation of radar
935 reflectivity factor together with lightning, showed a significant and positive impact on the
936 short-term precipitation forecasts (Federico et al., 2019).

937

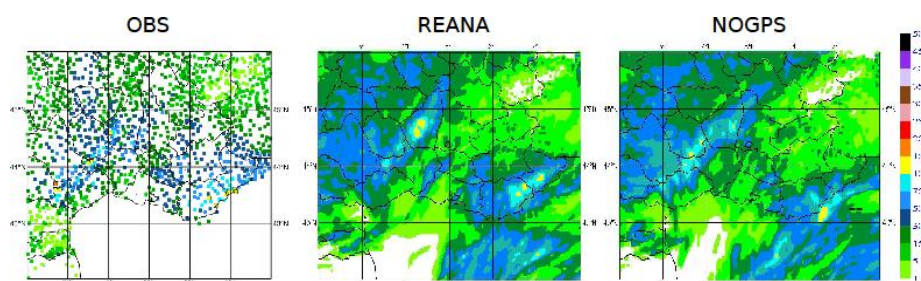


Figure 9: 24 hour accumulated precipitation (mm/24hr) between 06:00 UTC, 26 Oct. and 06:00 UTC, 27 Oct. 2012 over southern France (zoom over Cévennes area); observations (left panel), REANA (middle panel) and NOGPS (right panel) simulations.

4.4 Predictability and ensemble forecasts

Despite advances in numerical modelling and data assimilation, the prediction of HP and related floods remains challenging because predictability of intense convective systems is limited, and user expectations are very high given the impact of HPEs. Ensemble prediction techniques can provide solutions through the elaboration of probabilistic HPE warnings. Until the 2010s, regional ensemble prediction systems were mainly limited by the large computational costs of increasing the members resolution and the ensemble size. Ensemble forecasts become even more useful when post-processing techniques are applied to the precipitation fields, using statistical methods such as regression or analogues (Diomede et al., 2014), with some difficulties due to the geographically complex forecast error structures of Mediterranean precipitation, and to the need of preparing very long reforecast datasets in order to adequately sample the statistical behaviour of HPEs.

With the availability of more powerful computational resources, operational regional models started to reach the kilometeric resolution leading to physically more realistic convection-permitting ensemble prediction systems (CPEPS). Studies of HPE events (Nuisier et al., 2016) have shown the added value of CPEPS over deterministic approaches or lower resolution ensembles. The enhanced exchange of validation datasets during HyMeX facilitated the objective verification of this kind of result in several ensemble studies such as Roux et al. (2019).

Several studies in the framework of HyMeX have demonstrated that, besides sensitivity to synoptic scale forcing represented by lateral boundary condition (LBC) perturbations, CPEPS systems were sensitive to multiple error sources, which had to be sampled as



specific perturbation in the parameterization schemes. Some sensitivity of ensemble spread to the model physics (turbulence and microphysics schemes) was demonstrated in Hally et al. (2014), who used the HyMeX IOP6 and IOP7a forecast and observation dataset to show that LBC perturbations cannot be neglected, and that the relative importance of LBC and physics uncertainties is case-dependent, with physics uncertainty being more significant during weakly forced convective events. Vié et al. (2012) explored the impact of microphysical processes on CPEPS spread and found a relationship between precipitation evaporation and the uncertainty of cold pool formation, which can be relevant to predict the correct location of HPEs. Bouttier et al. (2015) found a beneficial impact of randomly perturbing surface fields such as SST or soil moisture: the high density of HyMeX SOP1 data gave statistical significance to these results, because the objective verification of ensembles at high resolution requires large observational datasets. Besides developing physics perturbation techniques, other ensemble approaches were tested in HyMeX case studies, based on different models or parameterization schemes. This multiphysics or multi-model technique was shown to be relevant to HPE events in several studies, such as Davolio et al. (2013), Hally et al. (2015), Ravazzani et al. (2016). Compared to other sources of uncertainty, the maximum impact of physics, multiphysics or surface perturbations tends to be observed at forecast ranges between a few hours and about one day, after which the CPEPS behaviour is usually dominated by the LBCs.

The specification of the ensemble LBCs can be optimized in terms of the HPE forecasts: Nuissier et al. (2012) showed that LBC member selection from a global ensemble, using a clustering technique, improves over a random selection. Marsigli et al. (2014) demonstrated that direct nesting into the ECMWF ensemble, instead of using an intermediate model, is beneficial despite the large resolution jump between the global and CP ensemble.

Initial condition perturbations using ensemble data assimilation systems were studied in Vié et al. (2012) and Bouttier et al. (2016). They found that initial condition perturbations are critical to achieve a correct CPEPS ensemble spread, typically during the first twelve hours of prediction, after which other perturbation sources (LBCs, surface and stochastic model perturbations) tend to dominate.

Verification of ensemble forecasts of HPEs can be overtaken using probabilistic scores, It greatly benefits from the large amount of observations available during the SOPs. Ensemble predictions can also be evaluated by their ability to drive ensembles of hydrological runoff models. Indeed, it was confirmed during HyMeX that although hydrological models suffer for their own uncertainties (Edouard et al., 2018), precipitation forecast



errors are the main sources of uncertainty for flood prediction. Many studies dealing with CPEPS also exploited precipitation forecasts to drive flood prediction systems. Among others, Roux et al. (2019) pointed out that enhancing the spread of HPE precipitation forecasts tends to help flood warnings by improving the detection of extreme HPE scenarios.

An emerging application of CPEPS forecasts consists in investigating the physical mechanisms that drive HPE events (and, possibly, the reasons behind forecast failures), as exemplified in the USA by Nielsen and Schumacher (2016). In the HyMeX framework, beside the above-mentioned studies on physical perturbations, importance of orographically driven low-level flows was confirmed using CPEPS in Hally et al. (2014) and Nuissier et al. (2016). Figure 10 shows an example for the IOP16 case.

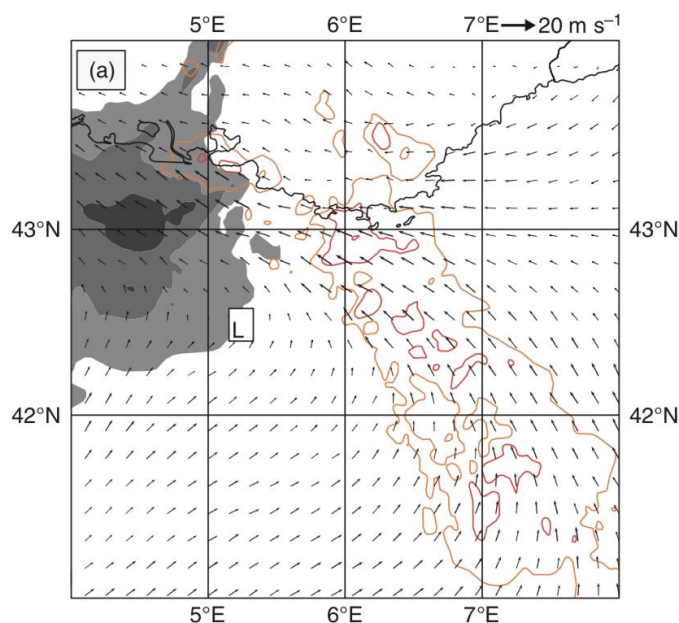


Figure 10: Lowest quartile of the mean sea-level pressure (shading), mean 10m wind (arrows) and mean moisture flux at 925hPa (solid lines: 80 and 100 g m s⁻²) valid at 12:00 UTC, 26 Oct. 2012 for the AROME-EPS ensemble. (credits: Nuissier et al., 2016)

5. Discussion



1023 The spatial complexity of the Mediterranean region, the intricacy of the dynamical and
1024 physical processes involved including the multiple interactions across scales, as well as
1025 the technical and observational limitations in the past have made HP understanding and
1026 modelling in the Mediterranean region a very challenging issue. To try to advance in this
1027 direction the Hydrological Cycle in the Mediterranean Experiment (HyMeX, 2010-2020)
1028 has put a major effort in investigating the predictability and evolution of extreme weather
1029 events. Within this framework and profiting from the state-of-the-art observational
1030 datasets and modelling capabilities lately available and developed within the
1031 programme, important achievements towards improved understanding of the
1032 mechanisms leading to HP in the WMed have been accomplished. In this paper we
1033 review the main advances and lessons learned during HyMeX, including results emerged
1034 from cross-disciplinary studies.

1035

1036 The unprecedented richness of observations and numerical experiments during HyMeX
1037 led to major achievements and the identification of primary needs for an improved
1038 understanding and predictability of HPE. Our better comprehension of the moist
1039 convergence role on MCS initiation over the sea, the first-time airborne observations of
1040 WCB, the high space-time resolution measurements of the 3-D fields of water vapour, or
1041 the testing of new convection-permitting ensembles, which provided new insights on
1042 HPE predictability and of forecast error sources, among others illustrate the main
1043 accomplishments achieved during HyMeX. Parallel to this, observational, modelling and
1044 knowledge gaps have been identified clearly indicating the needs for future applications.
1045 Sensitivity to soils and sea surface conditions with impacts on high-resolution forecasts
1046 pointed out the need to build and/or improve high-resolution coupled systems able to
1047 represent the full evolution of the soil and ocean conditions. The need of a higher number
1048 of observations, for example collected over the sea, thermodynamic profile
1049 measurements and wind on a high space-time resolution would have a major impact on
1050 forecasting capabilities, through the initialization of modelling systems, data assimilation
1051 and the definition of improved parameterization schemes for turbulence and convection.
1052 Also, open questions remain regarding access to large samples of HPE reforecasts, the
1053 representation of model error processes specific to HPE systems and persisting
1054 shortcomings in the real-time prediction of extreme precipitation events for flood
1055 warnings, among others. Furthermore, coordinated research efforts will be needed to
1056 address topics of multi-scale interactions, from large-scale dynamics to microphysical
1057 processes.

1058



1059 Along with the aforementioned achievements and demands, the continuous
1060 collaboration between scientific communities, e.g., oceanographers and meteorologists,
1061 and among scientific teams (ST) has been a priority and a success of the project. In fact
1062 coordinated efforts, in particular with the ST-lightning (Lightning and atmospheric
1063 electricity), ST-TIP (Towards integrated prediction of heavy precipitation, flash-floods
1064 and impacts), ST-ffv (Flash-floods and social vulnerabilities), and ST-medcyclones
1065 (Mediterranean Cyclones), through the development and use of common observation
1066 and modelling tools, and by sharing results and expertise, helped each other towards
1067 common goals. As illustration, aiming at a better understanding of processes leading to
1068 flash floods, as well as at their accurate modelling and forecasting, the ST-ffv actively
1069 contributed to the improvement of heavy rainfall prediction. Several recent
1070 multidisciplinary studies investigated the possibility to have an integrated modelling
1071 approach from heavy rainfall forecasting, to discharge prediction, to social impact.
1072 Methodologies of postflood field surveys based on interdisciplinary collaborations
1073 between hydrologists and social scientists have been proposed (Ruin et al., 2014; Borga
1074 et al., 2019). For instance, Papagiannaki et al. (2017) investigated the link between HP
1075 and impacts on the flash flood that occurred in October 2015 in Attica. The survey
1076 responses provided insights into risk perception and behavioral reactions relative to the
1077 space-time distribution of rainfall. Different possibilities of improving hydrometeorological
1078 forecasts have also been tested (Roux et al., 2020), pointing out the added value of
1079 ensemble strategies with respect to deterministic forecasts. Large meteorological
1080 ensemble spreads also allowed better threshold exceedance detection for flood warning.
1081 Furthermore, the rapid increase of total lightning flash rates has been found to be an
1082 important predictor for severe weather phenomena (e.g., Wu et al., 2018), which is
1083 closely related to the rapid increase of graupel concentration and updraft volumes in the
1084 mixed-phase layers of deep convective systems. Furthermore, many studies in the
1085 framework of the ST-lightning have been devoted to the examination of the relationship
1086 of lightning activity with microphysical properties of convective systems along their life
1087 cycle. During HyMeX SOP1, the HyMeX lightning mapping array network (HyLMA; Defer
1088 et al., 2015) was operated to locate and characterize the 3D lightning activity over the
1089 Cévenne-Vivarais area at flash, storm, and regional scales. This unique and
1090 comprehensive lightning data clearly showed the large potential for improving our
1091 knowledge about the cloud microphysics, especially the distribution and evolution of ice
1092 hydrometeors by taking advantage of cloud electrification. This challenging subject is
1093 expected to be further addressed in near future.

1094



1095 The increased computational capacity, the development of high-resolution convection-
1096 permitting models and the availability of state-of-the-art observations have demonstrated
1097 to be of pivotal importance to attain a better understanding and modelling of HP in the
1098 last decade. Nevertheless, still the availability of observational data on the analysis of,
1099 e.g., small-scale processes, remains a limiting factor that challenges progress in process
1100 understanding and model evaluation, particularly when trying to underpin results from
1101 high-resolution model experiments with corresponding observations. Additionally,
1102 evaluation is expected to continue in those recent investigation lines developed within
1103 the HyMeX programme, which have already demonstrated their usefulness for
1104 advancing prediction or knowledge of HPE, such as CPEPS systems or the development
1105 and availability of fully coupled soil-vegetation-atmosphere-ocean models. Furthermore,
1106 the benefit of working under the umbrella of a long-lasting international experiment such
1107 as HyMeX allowed an effective and fruitful exchange of information on challenges,
1108 experiences, and goals, exploited through numerous multidisciplinary research activities.
1109 These interdisciplinary efforts were crucial to come towards improved understanding of
1110 the mechanisms leading to HP in the WMed. The links and networks originated in the
1111 framework of HyMeX must continue and even be enlarged in the future to progress
1112 together towards more integrated approaches. Novel integrated multidisciplinary
1113 research partnerships based on cross-sectional collaborations will be indeed needed to
1114 bridge more efficient research on impacts.

1115

1116 **Code and Data Availability**

1117 Given this is a review publication, the data and code availability are provided in each of
1118 the referenced publications.

1119

1120 **Author contributions**

1121 All authors collaborated and contributed to drafting, reviewing, and editing the paper. In
1122 particular, SK coordinated the effort and wrote the original draft; SD contributed to the
1123 reviewing of the low-level dynamical processes; PDG contributed to the reviewing of the
1124 observational capabilities; CLB contributed to the reviewing of the air-sea coupling; EF
1125 contributed to the reviewing of the large-scale dynamics; NF contributed to the reviewing
1126 of data assimilation; KOL contributed to the reviewing of the low-level dynamical
1127 processes; DR contributed to the reviewing of improved parameterizations; BV



1128 contributed to the reviewing of the microphysics; FB contributed to the reviewing of the
1129 predictability and ensemble forecast.

1130

1131 **Competing Interests**

1132 The authors declare that they have no conflict of interest.

1133

1134 **Acknowledgements**

1135 This work is a contribution to the HyMeX programme, supported in France by MISTRALS
1136 (Météo-France, CNRS, INRAE) and the Agence Nationale de la Recherche (ANR
1137 MUSIC grant ANR-14-CE01-0014, ANR IODA-MED grant ANR-11-BS56-0005). We
1138 would like to thank all HyMeX contributors, and particularly to all members of the
1139 scientific-team heavy precipitation (ST-HP), more than 100 in the last 10 years, which
1140 have effectively participated in advancing knowledge regarding heavy precipitation in the
1141 Mediterranean region. Without their work this study would not be possible. We further
1142 acknowledge the HyMeX database developers and all data providers.
1143 We also thank all HyMeX scientific team coordinators for the close cooperation during
1144 these years. We acknowledge H  l  ne Roux and Eric Defer for their input on research
1145 activities of the ST-ffv and ST-lightning. The authors thank Marie-No  lle Bouin (CNRM
1146 & LOPS) who provided us MESO-NH simulation data related to IOP16a sensitivity to
1147 waves. The contribution of Paolo Di Girolamo to this work was possible based on the
1148 support from the Italian Ministry for Education, University and Research under the Grant
1149 OT4CLIMA and FISR2019_01711 CONCERNING.

1150

1151 **References**

1152

1153 Adirosi, E., Gorgucci, E., Baldini, L. and Tokay, A.: Evaluation of Gamma Raindrop Size
1154 Distribution Assumption through Comparison of Rain Rates of Measured and Radar-
1155 Equivalent Gamma DSD, Journal of Applied Meteorology and Climatology, 53(6), 1618–
1156 1635, doi:10.1175/jamc-d-13-0150.1, 2014.

1157

1158 Adirosi, E., Baldini, L., Lombardo, F., Russo, F., Napolitano, F., Volpi, E. and Tokay, A.:
1159 Comparison of different fittings of drop spectra for rainfall retrievals, Advances in Water
1160 Resources, 83, 55–67, doi:10.1016/j.advwatres.2015.05.009, 2015.

1161



- 1162 Adirosi, E., Baldini, L., Roberto, N., Gatlin, P. and Tokay, A.: Improvement of vertical
 1163 profiles of raindrop size distribution from micro rain radar using 2D video disdrometer
 1164 measurements, *Atmospheric Research*, 169, 404–415,
 1165 doi:10.1016/j.atmosres.2015.07.002, 2016.
- 1166
- 1167 Adler, B., Kalthoff, N., Kohler, M., Handwerker, J., Wieser, A., Corsmeier, U., Kottmeier,
 1168 C., Lambert, D. and Bock, O.: The variability of water vapour and pre-convective
 1169 conditions over the mountainous island of Corsica, *Quarterly Journal of the Royal*
 1170 *Meteorological Society*, 142, 335–346, doi:10.1002/qj.2545, 2015.
- 1171
- 1172 Augros, C., Caumont, O., Ducrocq, V., Gaussiat, N. and Tabary, P.: Comparisons
 1173 between S-, C- and X-band polarimetric radar observations and convective-scale
 1174 simulations of the HyMeX first special observing period, *Quarterly Journal of the Royal*
 1175 *Meteorological Society*, 142, 347–362, doi:10.1002/qj.2572, 2015.
- 1176
- 1177 Barthlott, C. and Kirshbaum, D. J.: Sensitivity of deep convection to terrain forcing over
 1178 Mediterranean islands, *Quarterly Journal of the Royal Meteorological Society*, 139(676),
 1179 1762–1779, doi:10.1002/qj.2089, 2013.
- 1180
- 1181 Barthlott, C., Adler, B., Kalthoff, N., Handwerker, J., Kohler, M. and Wieser, A.: The role
 1182 of Corsica in initiating nocturnal offshore convection, *Quarterly Journal of the Royal*
 1183 *Meteorological Society*, 142, 222–237, doi:10.1002/qj.2415, 2016.
- 1184
- 1185 Barthlott, C. and Davolio, S.: Mechanisms initiating heavy precipitation over Italy during
 1186 HyMeX Special Observation Period 1: a numerical case study using two mesoscale
 1187 models, *Quarterly Journal of the Royal Meteorological Society*, 142, 238–258,
 1188 doi:10.1002/qj.2630, 2016.
- 1189
- 1190 Bassi, C.: Modelli meteorologici ad alta risoluzione: simulazione di episodi di
 1191 precipitazione intensa in Liguria e Toscana durante la campagna HyMeX, Università di
 1192 Milano, <https://www.sba.unimi.it/en/thesis/49.html>, 2014.
- 1193
- 1194 Bastin, S., Drobinski, P., Chiriaco, M., Bock, O., Roehrig, R., Gallardo, C., Conte, D.,
 1195 Alonso, M. D., Li, L., Lionello, P. and Parracho, A. C.: Impact of humidity biases on light
 1196 precipitation occurrence: observations versus simulations, *Atmospheric Chemistry and*
 1197 *Physics*, 19(3), 1471–1490, doi:10.5194/acp-19-1471-2019, 2019.
- 1198



- 1199 Berthou, S., Mailler, S., Drobinski, P., Arsouze, T., Bastin, S., Béranger, K., Flaounas,
 1200 E., Brossier, C. L., Somot, S. and Stéfanon, M.: Influence of submonthly air-sea coupling
 1201 on heavy precipitation events in the Western Mediterranean basin, *Quarterly Journal of*
 1202 *the Royal Meteorological Society*, 142, 453–471, doi:10.1002/qj.2717, 2016.
- 1203
- 1204 Berthou, S., Kendon, E. J., Chan, S. C., Ban, N., Leutwyler, D., Schär, C. and Fosser,
 1205 G.: Pan-European climate at convection-permitting scale: a model intercomparison
 1206 study, *Climate Dynamics*, 55(1-2), 35–59, doi:10.1007/s00382-018-4114-6, 2018.
- 1207
- 1208 Bock, O., Bosser, P., Pacione, R., Nuret, M., Fourrié, N. and Parracho, A.: A high-quality
 1209 reprocessed ground-based GPS dataset for atmospheric process studies, radiosonde
 1210 and model evaluation, and reanalysis of HyMeX Special Observing Period, *Quarterly*
 1211 *Journal of the Royal Meteorological Society*, 142, 56–71, doi:10.1002/qj.2701, 2016.
- 1212
- 1213 Bonan, B., Albergel, C., Zheng, Y., Barbu, A. L., Fairbairn, D., Munier, S. and Calvet, J.-
 1214 C.: An ensemble square root filter for the joint assimilation of surface soil moisture and
 1215 leaf area index within the Land Data Assimilation System LDAS-Monde: application over
 1216 the Euro-Mediterranean region, *Hydrology and Earth System Sciences*, 24(1), 325–347,
 1217 doi:10.5194/hess-24-325-2020, 2020.
- 1218
- 1219 Borderies, M., Caumont, O., Delanoë, J., Ducrocq, V. and Fourrié, N.: Assimilation of
 1220 wind data from airborne Doppler cloud-profiling radar in a kilometre-scale NWP system,
 1221 *Natural Hazards and Earth System Sciences*, 19(4), 821–835, doi:10.5194/nhess-19-
 1222 821-2019, 2019a.
- 1223
- 1224 Borderies, M., Caumont, O., Delanoë, J., Ducrocq, V., Fourrié, N. and Marquet, P.:
 1225 Impact of airborne cloud radar reflectivity data assimilation on kilometre-scale numerical
 1226 weather prediction analyses and forecasts of heavy precipitation events, *Natural*
 1227 *Hazards and Earth System Sciences*, 19(4), 907–926, doi:10.5194/nhess-19-907-2019,
 1228 2019b.
- 1229
- 1230 Borga, M., Comiti, F., Ruin, I. and Marra, F.: Forensic analysis of flash flood response,
 1231 *WIREs Water*, 6(2), doi:10.1002/wat2.1338, 2019.
- 1232
- 1233 Bougeault, P., Binder, P., Buzzi, A., Dirks, R., Kuettner, J., Houze, R., Smith, R. B.,
 1234 Steinacker, R. and Volkert, H.: The MAP Special Observing Period, *Bulletin of the*



- 1235 American Meteorological Society, 82(3), 433–462, doi:10.1175/1520-
 1236 0477(2001)082<0433:tmsop>2.3.co;2, 2001.
- 1237
- 1238 Bouin, M.-N., Redelsperger, J.-L. and Brossier, C. L.: Processes leading to deep
 1239 convection and sensitivity to sea-state representation during HyMeX IOP8 heavy
 1240 precipitation event, Quarterly Journal of the Royal Meteorological Society,
 1241 143(707), 2600–2615, doi:10.1002/qj.3111, 2017.
- 1242
- 1243 Bouttier, F., Raynaud, L., Nuissier, O. and Ménétrier, B.: Sensitivity of the AROME
 1244 ensemble to initial and surface perturbations during HyMeX, Quarterly Journal of the
 1245 Royal Meteorological Society, 142, 390–403, doi:10.1002/qj.2622, 2015.
- 1246
- 1247 Bresson, E., Ducrocq, V., Nuissier, O., Ricard, D. and de Saint-Aubin, C. (2012),
 1248 Idealized numerical simulations of quasi-stationary convective systems over the
 1249 Northwestern Mediterranean complex terrain. Q.J.R. Meteorol. Soc., 138: 1751-1763.
 1250 <https://doi.org/10.1002/qj.1911>
- 1251
- 1252 Brossier, C. L., Arsouze, T., Béranger, K., Bouin, M.-N., Bresson, E., Ducrocq, V.,
 1253 Giordani, H., Nuret, M., Rainaud, R. and Taupier-Letage, I.: Ocean Mixed Layer
 1254 responses to intense meteorological events during HyMeX-SOP1 from a high-resolution
 1255 ocean simulation, Ocean Modelling, 84, 84–103, doi:10.1016/j.ocemod.2014.09.009,
 1256 2014.
- 1257
- 1258 Buzzi, A., Davolio, S., Malguzzi, P., Drofa, O. and Mastrangelo, D.: Heavy rainfall
 1259 episodes over Liguria in autumn 2011: numerical forecasting experiments, Natural
 1260 Hazards and Earth System Sciences, 14(5), 1325–1340, doi:10.5194/nhess-14-1325-
 1261 2014, 2014.
- 1262
- 1263 Caine, S., Lane, T. P., May, P. T., Jakob, C., Siems, S. T., Manton, M. J. and Pinto, J.:
 1264 Statistical Assessment of Tropical Convection-Permitting Model Simulations Using a
 1265 Cell-Tracking Algorithm, Monthly Weather Review, 141(2), 557–581, doi:10.1175/mwr-
 1266 d-11-00274.1, 2013.
- 1267
- 1268 Caldas-Álvarez, A., Khodayar, S. and Bock, O.: GPS – Zenith Total Delay assimilation
 1269 in different resolution simulations of a heavy precipitation event over southern France,
 1270 Advances in Science and Research, 14, 157–162, doi:10.5194/asr-14-157-2017, 2017.
- 1271



- 1272 Caldas-Alvarez, A. and Khodayar, S.: Assessing atmospheric moisture effects on heavy
 1273 precipitation during HyMeX IOP16 using GPS nudging and dynamical downscaling,
 1274 Natural Hazards and Earth System Sciences, 20(10), 2753–2776, doi:10.5194/nhess-
 1275 20-2753-2020, 2020.
- 1276
- 1277 Cavaleri, L., Bajo, M., Barbariol, F., Bastianini, M., Benetazzo, A., Bertotti, L., Chiggiato,
 1278 J., Davolio, S., Ferrarin, C., Magnusson, L., Papa, A., Pezzutto, P., Pomaro, A. and
 1279 Umgiesser, G.: The October 29, 2018 storm in Northern Italy – An exceptional event and
 1280 its modeling, Progress in Oceanography, 178, 102178,
 1281 doi:10.1016/j.pocean.2019.102178, 2019.
- 1282
- 1283 Chazette, P., Flamant, C., Raut, J.-C., Totems, J. and Shang, X.: Tropical moisture
 1284 enriched storm tracks over the Mediterranean and their link with intense rainfall in the
 1285 Cevennes-Vivarais area during HyMeX, Quarterly Journal of the Royal Meteorological
 1286 Society, 142, 320–334, doi:10.1002/qj.2674, 2015a.
- 1287
- 1288 Chazette, P., Flamant, C., Shang, X., Totems, J., Raut, J.-C., Doerenbecher, A.,
 1289 Ducrocq, V., Fourrié, N., Bock, O. and Cloché, S.: A multi-instrument and multi-model
 1290 assessment of atmospheric moisture variability over the western Mediterranean during
 1291 HyMeX, Quarterly Journal of the Royal Meteorological Society, 142, 7–22,
 1292 doi:10.1002/qj.2671, 2015b.
- 1293
- 1294 Chazette, P., Totems, J., Ancellet, G., Pelon, J. and Sicard, M.: Temporal consistency of
 1295 lidar observations during aerosol transport events in the framework of the
 1296 ChArMEx/ADRIED campaign at Minorca in June 2013, Atmospheric Chemistry and
 1297 Physics, 16(5), 2863–2875, doi:10.5194/acp-16-2863-2016, 2016.
- 1298
- 1299 Clark, P., Roberts, N., Lean, H., Ballard, S. P. and Charlton-Perez, C.: Convection-
 1300 permitting models: a step-change in rainfall forecasting, Meteorological Applications,
 1301 23(2), 165–181, doi:10.1002/met.1538, 2016.
- 1302
- 1303 Colmet-Daage, A., Sanchez-Gomez, E., Ricci, S., Llovel, C., Estupina, V. B., Quintana-
 1304 Seguí, P., Llasat, M. C. and Servat, E.: Evaluation of uncertainties in mean and extreme
 1305 precipitation under climate changes for northwestern Mediterranean watersheds from
 1306 high-resolution Med and Euro-CORDEX ensembles, doi:10.5194/hess-2017-49, 2017.
- 1307



- 1308 Coppola, E., Sobolowski, S., Pichelli, E., Raffaele, F., Ahrens, B., Anders, I., Ban, N.,
 1309 Bastin, S., Belda, M., Belusic, D., Caldas-Alvarez, A., Cardoso, R. M., Davolio, S.,
 1310 Dobler, A., Fernandez, J., Fita, L., Fumiere, Q., Giorgi, F., Goergen, K., Güttler, I.,
 1311 Halenka, T., Heinzeller, D., Hodnebrog, Ø., Jacob, D., Kartsios, S., Katragkou, E.,
 1312 Kendon, E., Khodayar, S., Kunstmann, H., Knist, S., Lavín-Gullón, A., Lind, P., Lorenz,
 1313 T., Maraun, D., Marelle, L., van Meijgaard, E., Milovac, J., Myhre, G., Panitz, H.-J.,
 1314 Piazza, M., Raffa, M., Raub, T., Rockel, B., Schär, C., Sieck, K., Soares, P. M. M., Somot,
 1315 S., Srnec, L., Stocchi, P., Tölle, M. H., Truhetz, H., Vautard, R., de Vries, H. and Warrach-
 1316 Sagi, K.: A first-of-its-kind multi-model convection permitting ensemble for investigating
 1317 convective phenomena over Europe and the Mediterranean, *Climate Dynamics*, 55(1-2),
 1318 3–34, doi:10.1007/s00382-018-4521-8, 2018.
- 1319
- 1320 Corsmeier, U., Hankers, R. and Wieser, A.: Airborne turbulence measurements in the
 1321 lower troposphere onboard the research aircraft Dornier 128-6, *D-IBUF,*
 1322 *Meteorologische Zeitschrift*, 10(4), 315–329, doi:10.1127/0941-2948/2001/0010-0315,
 1323 2001.
- 1324
- 1325 Davolio, S., Mastrangelo, D., Miglietta, M. M., Drofa, O., Buzzi, A. and Malguzzi, P.: High
 1326 resolution simulations of a flash flood near Venice, *Natural Hazards and Earth System*
 1327 *Sciences*, 9(5), 1671–1678, doi:10.5194/nhess-9-1671-2009, 2009.
- 1328
- 1329 Davolio, S., Miglietta, M. M., Diomede, T., Marsigli, C. and Montani, A.: A flood episode
 1330 in northern Italy: multi-model and single-model mesoscale meteorological ensembles for
 1331 hydrological predictions, *Hydrology and Earth System Sciences*, 17(6), 2107–2120,
 1332 doi:10.5194/hess-17-2107-2013, 2013.
- 1333
- 1334 Davolio, S., Silvestro, F. and Malguzzi, P.: Effects of Increasing Horizontal Resolution in
 1335 a Convection-Permitting Model on Flood Forecasting: The 2011 Dramatic Events in
 1336 Liguria, Italy, *Journal of Hydrometeorology*, 16(4), 1843–1856, doi:10.1175/jhm-d-14-
 1337 0094.1, 2015.
- 1338
- 1339 Davolio, S., Henin, R., Stocchi, P. and Buzzi, A.: Bora wind and heavy persistent
 1340 precipitation: atmospheric water balance and role of air-sea fluxes over the Adriatic Sea,
 1341 *Quarterly Journal of the Royal Meteorological Society*, 143(703), 1165–1177,
 1342 doi:10.1002/qj.3002, 2017.
- 1343



- 1344 Davolio, S., Della Fera, S., Laviola, S., Miglietta, M. M. and Levizzani, V.: Heavy
 1345 Precipitation over Italy from the Mediterranean Storm "in October 2018: Assessing the
 1346 Role of an Atmospheric River, *Monthly Weather Review*, 148(9), 3571–3588,
 1347 doi:10.1175/mwr-d-20-0021.1, 2020.
- 1348
- 1349 Dayan, U., Nissen, K. and Ulbrich, U.: Review Article: Atmospheric conditions inducing
 1350 extreme precipitation over the eastern and western Mediterranean, *Natural Hazards and*
 1351 *Earth System Sciences*, 15(11), 2525–2544, doi:10.5194/nhess-15-2525-2015, 2015.
- 1352
- 1353 Defer, E., Pinty, J.-P., Coquillat, S., Martin, J.-M., Prieur, S., Soula, S., Richard, E., Rison,
 1354 W., Krehbiel, P., Thomas, R., Rodeheffer, D., Vergeiner, C., Malaterre, F., Pedebay, S.,
 1355 Schulz, W., Farges, T., Gallin, L.-J., Ortéga, P., Ribaud, J.-F., Anderson, G., Betz, H.-D.,
 1356 Meneux, B., Kotroni, V., Lagouvardos, K., Roos, S., Ducrocq, V., Roussot, O., Labatut,
 1357 L. and Molinié, G.: An overview of the lightning and atmospheric electricity observations
 1358 collected in southern France during the HYdrological cycle in Mediterranean EXperiment
 1359 (HyMeX), *Special Observation Period 1, Atmospheric Measurement Techniques*, 8(2),
 1360 649–669, doi:10.5194/amt-8-649-2015, 2015.
- 1361
- 1362 Diomede, T., Marsigli, C., Montani, A., Nerozzi, F. and Paccagnella, T.: Calibration of
 1363 Limited-Area Ensemble Precipitation Forecasts for Hydrological Predictions, *Monthly*
 1364 *Weather Review*, 142(6), 2176–2197, doi:10.1175/mwr-d-13-00071.1, 2014.
- 1365
- 1366 Doerenbecher, A., Basdevant, C., Drobinski, P., Durand, P., Fesquet, C., Bernard, F.,
 1367 Cocquerez, P., Verdier, N. and Vargas, A.: Low-Atmosphere Drifting Balloons: Platforms
 1368 for Environment Monitoring and Forecast Improvement, *Bulletin of the American*
 1369 *Meteorological Society*, 97(9), 1583–1599, doi:10.1175/bams-d-14-00182.1, 2016.
- 1370
- 1371 Doocy, S., Daniels, A., Murray, S. and Kirsch, T. D.: The Human Impact of Floods: a
 1372 Historical Review of Events 1980-2009 and Systematic Literature Review, *PLoS*
 1373 *Currents*, doi:10.1371/currents.dis.f4deb457904936b07c09daa98ee8171a, 2013.
- 1374
- 1375 Draxler, R. R. and Hess, G. D.: An overview of the HYSPLIT_4 modelling system for
 1376 trajectories, dispersion and deposition, *Aust. Met. Mag.*, 47, 295–308, 1998.
- 1377
- 1378 Drobinski, P., Ducrocq, V., Alpert, P., Anagnostou, E., Béranger, K., Borga, M., Braud,
 1379 I., Chanzy, A., Davolio, S., Delrieu, G., Estournel, C., Boubrahmi, N. F., Font, J., Grubišić,
 1380 V., Gualdi, S., Homar, V., Ivančan-Picek, B., Kottmeier, C., Kotroni, V., Lagouvardos, K.,



- 1381 Lionello, P., Llasat, M. C., Ludwig, W., Lutoff, C., Mariotti, A., Richard, E., Romero, R.,
 1382 Rotunno, R., Roussot, O., Ruin, I., Somot, S., Taupier-Letage, I., Tintore, J., Uijlenhoet,
 1383 R. and Wernli, H.: HyMeX: A 10-Year Multidisciplinary Program on the Mediterranean
 1384 Water Cycle, *Bulletin of the American Meteorological Society*, 95(7), 1063–1082,
 1385 doi:10.1175/bams-d-12-00242.1, 2014.
- 1386
- 1387 Drobinski, P., Silva, N. D., Panthou, G., Bastin, S., Muller, C., Ahrens, B., Borga, M.,
 1388 Conte, D., Fosser, G., Giorgi, F., Güttler, I., Kotroni, V., Li, L., Morin, E., Öno, B.,
 1389 Quintana-Segui, P., Romera, R. and Torma, C. Z.: Scaling precipitation extremes with
 1390 temperature in the Mediterranean: past climate assessment and projection in
 1391 anthropogenic scenarios, *Climate Dynamics*, 51(3), 1237–1257, doi:10.1007/s00382-
 1392 016-3083-x, 2016.
- 1393
- 1394 Ducrocq, V., Nuissier, O., Ricard, D., Lebeaupin, C. and Thouvenin, T.: A numerical
 1395 study of three catastrophic precipitating events over southern France. II: Mesoscale
 1396 triggering and stationarity factors, *Quarterly Journal of the Royal Meteorological Society*,
 1397 134(630), 131–145, doi:10.1002/qj.199, 2008.
- 1398
- 1399 Ducrocq, V., Braud, I., Davolio, S., Ferretti, R., Flamant, C., Jansa, A., Kalthoff, N.,
 1400 Richard, E., Taupier-Letage, I., Ayral, P.-A., Belamari, S., Berne, A., Borga, M.,
 1401 Boudevillain, B., Bock, O., Boichard, J.-L., Bouin, M.-N., Bousquet, O., Bouvier, C.,
 1402 Chiggiato, J., Cimini, D., Corsmeier, U., Coppola, L., Cocquerez, P., Defer, E., Delanoë,
 1403 J., Girolamo, P. D., Doerenbecher, A., Drobinski, P., Dufournet, Y., Fourrié, N., Gourley,
 1404 J. J., Labatut, L., Lambert, D., Coz, J. L., Marzano, F. S., Molinié, G., Montani, A., Nord,
 1405 G., Nuret, M., Ramage, K., Rison, W., Roussot, O., Said, F., Schwarzenboeck, A.,
 1406 Testor, P., Baelen, J. V., Vincendon, B., Aran, M. and Tamayo, J.: HyMeX-SOP1: The
 1407 Field Campaign Dedicated to Heavy Precipitation and Flash Flooding in the
 1408 Northwestern Mediterranean, *Bulletin of the American Meteorological Society*, 95(7),
 1409 1083–1100, doi:10.1175/bams-d-12-00244.1, 2014.
- 1410
- 1411 Duffourg, F. and Ducrocq, V.: Origin of the moisture feeding the Heavy Precipitating
 1412 Systems over Southeastern France, *Natural Hazards and Earth System Sciences*, 11(4),
 1413 1163–1178, doi:10.5194/nhess-11-1163-2011, 2011.
- 1414
- 1415 Duffourg, F. and Ducrocq, V.: Assessment of the water supply to Mediterranean heavy
 1416 precipitation: a method based on finely designed water budgets, *Atmospheric Science*
 1417 *Letters*, 14(3), 133–138, doi:10.1002/asl2.429, 2013.



- 1418
- 1419 Duffourg, F., Nuissier, O., Ducrocq, V., Flamant, C., Chazette, P., Delanoë, J.,
 1420 Doerenbecher, A., Fourrié, N., Girolamo, P. D., Lac, C., Legain, D., Martinet, M., Saïd,
 1421 F. and Bock, O.: Offshore deep convection initiation and maintenance during the HyMeX
 1422 IOP 16a heavy precipitation event, *Quarterly Journal of the Royal Meteorological*
 1423 *Society*, 142, 259–274, doi:10.1002/qj.2725, 2016.
- 1424
- 1425 Duffourg, F., Lee, K.-O., Ducrocq, V., Flamant, C., Chazette, P. and Girolamo, P. D.:
 1426 Role of moisture patterns in the backbuilding formation of HyMeX IOP13 heavy
 1427 precipitation systems, *Quarterly Journal of the Royal Meteorological Society*, 144(710),
 1428 291–303, doi:10.1002/qj.3201, 2018.
- 1429
- 1430 Edouard, S., Vincendon, B. and Ducrocq, V.: Ensemble-based flash-flood modelling:
 1431 Taking into account hydrodynamic parameters and initial soil moisture uncertainties,
 1432 *Journal of Hydrology*, 560, 480–494, doi:10.1016/j.jhydrol.2017.04.048, 2018.
- 1433
- 1434 Federico, S., Torcasio, R. C., Avolio, E., Caumont, O., Montopoli, M., Baldini, L., Vulpiani,
 1435 G. and Dietrich, S.: The impact of lightning and radar reflectivity factor data assimilation
 1436 on the very short-term rainfall forecasts of RAMS@ISAC: application to two case studies
 1437 in Italy, *Natural Hazards and Earth System Sciences*, 19(8), 1839–1864,
 1438 doi:10.5194/nhess-19-1839-2019, 2019.
- 1439
- 1440 Fiori, E., Ferraris, L., Molini, L., Siccardi, F., Kranzlmüller, D. and Parodi, A.: Triggering
 1441 and evolution of a deep convective system in the Mediterranean Sea: modelling and
 1442 observations at a very fine scale, *Quarterly Journal of the Royal Meteorological Society*,
 1443 143(703), 927–941, doi:10.1002/qj.2977, 2017.
- 1444
- 1445 Flaounas, E., Raveh-Rubin, S., Wernli, H., Drobinski, P. and Bastin, S.: The dynamical
 1446 structure of intense Mediterranean cyclones, *Climate Dynamics*, 44(9-10), 2411–2427,
 1447 doi:10.1007/s00382-014-2330-2, 2014.
- 1448
- 1449 Flaounas, E., Lagouvardos, K., Kotroni, V., Claud, C., Delanoë, J., Flamant, C.,
 1450 Madonna, E. and Wernli, H.: Processes leading to heavy precipitation associated with
 1451 two Mediterranean cyclones observed during the HyMeX SOP1, *Quarterly Journal of the*
 1452 *Royal Meteorological Society*, 142, 275–286, doi:10.1002/qj.2618, 2015.
- 1453



- 1454 Flaounas, E., Luca, A. D., Drobinski, P., Mailler, S., Arsouze, T., Bastin, S., Beranger, K.
 1455 and Brossier, C. L.: Cyclone contribution to the Mediterranean Sea water budget, *Climate*
 1456 *Dynamics*, 46(3-4), 913–927, doi:10.1007/s00382-015-2622-1, 2015b.
- 1457
- 1458 Flaounas, E., Kotroni, V., Lagouvardos, K., Gray, S. L., Rysman, J.-F. and Claud, C.:
 1459 Heavy rainfall in Mediterranean cyclones. Part I: contribution of deep convection and
 1460 warm conveyor belt, *Climate Dynamics*, 50(7-8), 2935–2949, doi:10.1007/s00382-017-
 1461 3783-x, 2017.
- 1462
- 1463 Flaounas, E., Fita, L., Lagouvardos, K. and Kotroni, V.: Heavy rainfall in Mediterranean
 1464 cyclones, Part II: Water budget, precipitation efficiency and remote water sources,
 1465 *Climate Dynamics*, 53(5-6), 2539–2555, doi:10.1007/s00382-019-04639-x, 2019.
- 1466
- 1467 Fosser, G., Khodayar, S. and Berg, P.: Benefit of convection permitting climate model
 1468 simulations in the representation of convective precipitation, *Climate Dynamics*, 44(1-2),
 1469 45–60, doi:10.1007/s00382-014-2242-1, 2014.
- 1470
- 1471 Fourrié, N., Bresson, É., Nuret, M., Jany, C., Brousseau, P., Doerenbecher, A., Kreitz,
 1472 M., Nuissier, O., Sevault, E., Bénichou, H., Amodei, M. and Pouponneau, F.: AROME-
 1473 WMED, a real-time mesoscale model designed for the HyMeX special observation
 1474 periods, *Geoscientific Model Development*, 8(7), 1919–1941, doi:10.5194/gmd-8-1919-
 1475 2015, 2015.
- 1476
- 1477 Fourrié, N., Nuret, M., Brousseau, P., Caumont, O., Doerenbecher, A., Wattrelot, E.,
 1478 Moll, P., Bénichou, H., Puech, D., Bock, O., Bosser, P., Chazette, P., Flamant, C.,
 1479 Girolamo, P. D., Richard, E. and Saïd, F.: The AROME-WMED reanalyses of the first
 1480 special observation period of the Hydrological cycle in the Mediterranean experiment
 1481 (HyMeX), *Geoscientific Model Development*, 12(7), 2657–2678, doi:10.5194/gmd-12-
 1482 2657-2019, 2019.
- 1483
- 1484 Fourrié, N., Nuret, M., Brousseau, P. and Caumont, O.: Data assimilation impact studies
 1485 with the AROME-WMED reanalysis of the first special observation period of the
 1486 Hydrological cycle in the Mediterranean Experiment, *Natural Hazards and Earth System*
 1487 *Sciences*, 21(1), 463–480, doi:10.5194/nhess-21-463-2021, 2021.
- 1488
- 1489 Fresnay, S., Hally, A., Garnaud, C., Richard, E. and Lambert, D.: Heavy precipitation
 1490 events in the Mediterranean: sensitivity to cloud physics parameterisation uncertainties,



- 1491 Natural Hazards and Earth System Sciences, 12(8), 2671–2688, doi:10.5194/nhess-12-
 1492 2671-2012, 2012.
- 1493
- 1494 Fumière, Q., Déqué, M., Nuissier, O., Somot, S., Alias, A., Caillaud, C., Laurantin, O.
 1495 and Seity, Y.: Extreme rainfall in Mediterranean France during the fall: added value of
 1496 the CNRM-AROME Convection-Permitting Regional Climate Model, *Climate Dynamics*,
 1497 55(1-2), 77–91, doi:10.1007/s00382-019-04898-8, 2019.
- 1498
- 1499 Funatsu, B. M., Claud, C. and Chaboureaud, J.-P.: A 6-year AMSU-based climatology of
 1500 upper-level troughs and associated precipitation distribution in the Mediterranean region,
 1501 *Journal of Geophysical Research*, 113(D15), doi:10.1029/2008jd009918, 2008.
- 1502
- 1503 Galanaki, E., Flaounas, E., Kotroni, V., Lagouvardos, K. and Argiriou, A.: Lightning
 1504 activity in the Mediterranean: quantification of cyclones contribution and relation to their
 1505 intensity, *Atmospheric Science Letters*, 17(9), 510–516, doi:10.1002/asl.685, 2016.
- 1506
- 1507 Gao, X., Pal, J. S. and Giorgi, F.: Projected changes in mean and extreme precipitation
 1508 over the Mediterranean region from a high resolution double nested RCM simulation,
 1509 *Geophysical Research Letters*, 33(3), doi:10.1029/2005gl024954, 2006.
- 1510
- 1511 Giorgi, F.: Climate change hot-spots, *Geophysical Research Letters*, 33(8),
 1512 doi:10.1029/2006gl025734, 2006.
- 1513
- 1514 Giorgi, F., Raffaele, F. and Coppola, E.: The response of precipitation characteristics to
 1515 global warming from climate projections, *Earth System Dynamics*, 10(1), 73–89,
 1516 doi:10.5194/esd-10-73-2019, 2019.
- 1517
- 1518 Giovannini, L., Davolio, S., Zaramella, M., Zardi, D. and Borga, M.: Multi-model
 1519 convection-resolving simulations of the October 2018 Vaia storm over Northeastern Italy,
 1520 *Atmospheric Research*, 253, 105455, doi:10.1016/j.atmosres.2021.105455, 2021.
- 1521
- 1522 Gires, A., Tchiguirinskaia, I., Schertzer, D. and Berne, A.: 2DVD Data Revisited:
 1523 Multifractal Insights into Cuts of the Spatiotemporal Rainfall Process, *Journal of*
 1524 *Hydrometeorology*, 16(2), 548–562, doi:10.1175/jhm-d-14-0127.1, 2015.
- 1525
- 1526 Di Girolamo, P., Summa, D., Lin, R.-F., Maestri, T., Rizzi, R. and Masiello, G.: UV Raman
 1527 lidar measurements of relative humidity for the characterization of cirrus cloud



- 1528 microphysical properties, *Atmospheric Chemistry and Physics*, 9(22), 8799–8811,
 1529 doi:10.5194/acp-9-8799-2009, 2009.
- 1530
- 1531 Di Girolamo, P., Flamant, C., Cacciani, M., Summa, D., Stelitano, D., Richard, E.,
 1532 Ducrocq, V., Fourrie, N. and Said, F.: Lidar observations of low-level wind reversals over
 1533 the Gulf of Lion and characterization of their impact on the water vapour variability,
 1534 Author(s), 2017.
- 1535
- 1536 Grams, C. M., Wernli, H., Böttcher, M., Čampa, J., Corsmeier, U., Jones, S. C., Keller,
 1537 J. H., Lenz, C.-J. and Wiegand, L.: The key role of diabatic processes in modifying the
 1538 upper-tropospheric wave guide: a North Atlantic case-study, *Quarterly Journal of the*
 1539 *Royal Meteorological Society*, 137(661), 2174–2193, doi:10.1002/qj.891, 2011.
- 1540
- 1541 Grazioli, J., Tuia, D. and Berne, A.: Hydrometeor classification from polarimetric radar
 1542 measurements: a clustering approach, *Atmospheric Measurement Techniques*, 8(1),
 1543 149–170, doi:10.5194/amt-8-149-2015, 2015.
- 1544
- 1545 Grazzini, F., Craig, G. C., Keil, C., Antolini, G. and Pavan, V.: Extreme precipitation
 1546 events over northern Italy. Part I: A systematic classification with machine-learning
 1547 techniques, *Quarterly Journal of the Royal Meteorological Society*, 146(726), 69–85,
 1548 doi:10.1002/qj.3635, 2019.
- 1549
- 1550 Hachani, S., Boudevillain, B., Delrieu, G. and Bargaoui, Z.: Drop Size Distribution
 1551 Climatology in Cévennes-Vivarais Region, France, *Atmosphere*, 8(12), 233,
 1552 doi:10.3390/atmos8120233, 2017.
- 1553
- 1554 Hally, A., Richard, E. and Ducrocq, V.: An ensemble study of HyMeX IOP6 and IOP7a:
 1555 sensitivity to physical and initial and boundary condition uncertainties, *Natural Hazards*
 1556 *and Earth System Sciences*, 14(5), 1071–1084, doi:10.5194/nhess-14-1071-2014, 2014.
- 1557
- 1558 Hally, A., Caumont, O., Garrote, L., Richard, E., Weerts, A., Delogu, F., Fiori, E., Rebora,
 1559 N., Parodi, A., Mihalović, A., Ivković, M., Dekić, L., van Verseveld, W., Nuissier, O.,
 1560 Ducrocq, V., Galizia, D. D. A., Danovaro, E. and Clematis, A.: Hydrometeorological multi-
 1561 model ensemble simulations of the 4 November 2011 flash flood event in Genoa, Italy,
 1562 in the framework of the DRIHM project, *Natural Hazards and Earth System Sciences*,
 1563 15(3), 537–555, doi:10.5194/nhess-15-537-2015, 2015.
- 1564



- 1565 Hawcroft, M. K., Shaffrey, L. C., Hodges, K. I. and Dacre, H. F.: How much Northern
 1566 Hemisphere precipitation is associated with extratropical cyclones?, *Geophysical*
 1567 *Research Letters*, 39(24), doi:10.1029/2012gl053866, 2012.
- 1568
- 1569 Helgert, S. and Khodayar, S.: Improvement of the soil-atmosphere interactions and
 1570 subsequent heavy precipitation modelling by enhanced initialization using remotely
 1571 sensed 1 km soil moisture information, *Remote Sensing of Environment*, 246, 111812,
 1572 doi:10.1016/j.rse.2020.111812, 2020.
- 1573
- 1574 Hertig, E., Trambly, Y., Romberg, K., Kaspar-Ott, I. and Merckenschlager, C.: The impact
 1575 of soil moisture on precipitation downscaling in the Euro-Mediterranean area, *Climate*
 1576 *Dynamics*, 52(5-6), 2869–2884, doi:10.1007/s00382-018-4304-2, 2018.
- 1577
- 1578 Homar, V., Ramis, C., Romero, R., Alonso, S., Garcia-Moya, J. A. and Alarcon, M.: A
 1579 Case of Convection Development over the Western Mediterranean Sea: A Study through
 1580 Numerical Simulations, *Meteorology and Atmospheric Physics*, 71(3-4), 169–188,
 1581 doi:10.1007/s007030050054, 1999.
- 1582
- 1583 IPCC: Climate Change 2013: The Physical Science Basis. Contribution of Working
 1584 Group I to the Fifth Assessment Report of the Intergovernmental Panel on Climate
 1585 Change [Stocker, T.F., D. Qin, G.-K. Plattner, M. Tignor, S.K. Allen, J. Boschung, A.
 1586 Nauels, Y. Xia, V. Bex and P.M. Midgley (eds.)], edited by I. P. on Climate Change,
 1587 Cambridge University Press., 2009.
- 1588
- 1589 Jacob, D., Petersen, J., Eggert, B., Alias, A., Christensen, O. B., Bouwer, L. M., Braun,
 1590 A., Colette, A., Déqué, M., Georgievski, G., Georgopoulou, E., Gobiet, A., Menut, L.,
 1591 Nikulin, G., Haensler, A., Hempelmann, N., Jones, C., Keuler, K., Kovats, S., Kröner, N.,
 1592 Kotlarski, S., Kriegsman, A., Martin, E., van Meijgaard, E., Moseley, C., Pfeifer, S.,
 1593 Preuschmann, S., Radermacher, C., Radtke, K., Rechid, D., Rounsevell, M.,
 1594 Samuelsson, P., Somot, S., Soussana, J.-F., Teichmann, C., Valentini, R., Vautard, R.,
 1595 Weber, B. and Yiou, P.: EURO-CORDEX: new high-resolution climate change
 1596 projections for European impact research, *Regional Environmental Change*, 14(2), 563–
 1597 578, doi:10.1007/s10113-013-0499-2, 2013.
- 1598
- 1599 Jansa, A., Genoves, A., Picornell, M. A., Campins, J., Riosalido, R. and Carretero, O.:
 1600 Western Mediterranean cyclones and heavy rain. Part 2: Statistical approach,
 1601 *Meteorological Applications*, 8(1), 43–56, doi:10.1017/s1350482701001049, 2001.



1602
 1603 Jianyun, G., Ziwang, D. and Xiaolan, Z.: Spatial/temporal features of drought/flood in
 1604 Fujian for the past 4 decades, *Journal of Tropical Meteorology*, 22(5), 491–497, 2006.
 1605
 1606 Kagkara, C., Wobrock, W., Planche, C. and Flossmann, A. I.: The sensitivity of intense
 1607 rainfall to aerosol particle loading – a comparison of bin-resolved microphysics modelling
 1608 with observations of heavy precipitation from HyMeX IOP7a, *Natural Hazards and Earth*
 1609 *System Sciences*, 20(5), 1469–1483, doi:10.5194/nhess-20-1469-2020, 2020.
 1610
 1611 Kalthoff, N., Adler, B., Wieser, A., Kohler, M., Träumner, K., Handwerker, J., Corsmeier,
 1612 U., Khodayar, S., Lambert, D., Kopmann, A., Kunka, N., Dick, G., Ramatschi, M.,
 1613 Wickert, J. and Kottmeier, C.: KITcube a mobile observation platform for convection
 1614 studies deployed during HyMeX, *Meteorologische Zeitschrift*, 22(6), 633–647,
 1615 doi:10.1127/0941-2948/2013/0542, 2013.
 1616
 1617 Khodayar, S., Czajka, B., Caldas-Alvarez, A., Helgert, S., Flamant, C., Girolamo, P. D.,
 1618 Bock, O. and Chazette, P.: Multi-scale observations of atmospheric moisture variability
 1619 in relation to heavy precipitating systems in the northwestern Mediterranean during
 1620 HyMeX IOP12, *Quarterly Journal of the Royal Meteorological Society*, 144(717), 2761–
 1621 2780, doi:10.1002/qj.3402, 2018.
 1622
 1623 Khodayar, S., Fosser, G., Berthou, S., Davolio, S., Drobinski, P., Ducrocq, V., Ferretti,
 1624 R., Nuret, M., Pichelli, E., Richard, E. and Bock, O.: A seamless weather-climate multi-
 1625 model intercomparison on the representation of a high impact weather event in the
 1626 western Mediterranean: HyMeX IOP12, *Quarterly Journal of the Royal Meteorological*
 1627 *Society*, 142, 433–452, doi:10.1002/qj.2700, 2016a.
 1628
 1629 Khodayar, S., Kalthoff, N. and Kottmeier, C.: Atmospheric conditions associated with
 1630 heavy precipitation events in comparison to seasonal means in the western
 1631 mediterranean region, *Climate Dynamics*, 51(3), 951–967, doi:10.1007/s00382-016-
 1632 3058-y, 2016b.
 1633
 1634 Khodayar, S., Raff, F., Kalthoff, N. and Bock, O.: Diagnostic study of a high-precipitation
 1635 event in the Western Mediterranean: adequacy of current operational networks,
 1636 *Quarterly Journal of the Royal Meteorological Society*, 142, 72–85, doi:10.1002/qj.2600,
 1637 2015.
 1638



- 1639 Kirshbaum, D. J., Adler, B., Kalthoff, N., Barthlott, C. and Serafin S.: Moist orographic
 1640 convection: Physical mechanisms and links to surface-exchange processes,
 1641 Atmosphere, 9(3):80. <https://doi.org/10.3390/atmos9030080>, 2018.
- 1642
- 1643 Krichak, S. O., Feldstein, S. B., Alpert, P., Gualdi, S., Scoccimarro, E. and Yano, J.-I.:
 1644 Discussing the role of tropical and subtropical moisture sources in extreme precipitation
 1645 events in the Mediterranean region from a climate change perspective,
 1646 doi:10.5194/nhessd-3-3983-2015, 2015.
- 1647
- 1648 Lebeaupin-, C., Ducrocq, V. and Giordani, H.: Sensitivity of torrential rain events to the
 1649 sea surface temperature based on high-resolution numerical forecasts, Journal of
 1650 Geophysical Research, 111(D12), doi:10.1029/2005jd006541, 2006.
- 1651
- 1652 Lebeaupin-Brossier, C., Bastin, S., Béranger, K. and Drobinski, P.: Regional mesoscale
 1653 air–sea coupling impacts and extreme meteorological events role on the Mediterranean
 1654 Sea water budget, Climate Dynamics, 44(3-4), 1029–1051, doi:10.1007/s00382-014-
 1655 2252-z, 2014.
- 1656 Lee, K.-O., Flamant, C., Ducrocq, V., Duffourg, F., Fourrié, N. and Davolio, S.:
 1657 Convective initiation and maintenance processes of two back-building mesoscale
 1658 convective systems leading to heavy precipitation events in Southern Italy during HyMeX
 1659 IOP 13, Quarterly Journal of the Royal Meteorological Society, 142(700), 2623–2635,
 1660 doi:10.1002/qj.2851, 2016.
- 1661
- 1662 Lee, K.-O., Flamant, C., Ducrocq, V., Duffourg, F., Fourrié, N., Delanoë, J. and Bech, J.:
 1663 Initiation and development of a mesoscale convective system in the Ebro River Valley
 1664 and related heavy precipitation over northeastern Spain during HyMeX IOP 15a,
 1665 Quarterly Journal of the Royal Meteorological Society, 143(703), 942–956,
 1666 doi:10.1002/qj.2978, 2017.
- 1667
- 1668 Lee, K.-O., Flamant, C., Duffourg, F., Ducrocq, V. and Chaboureaud, J.-P.: Impact of
 1669 upstream moisture structure on a back-building convective precipitation system in south-
 1670 eastern France during HyMeX IOP13, Atmospheric Chemistry and Physics, 18(23),
 1671 16845–16862, doi:10.5194/acp-18-16845-2018, 2018.
- 1672
- 1673 Lee, K.-O., Aemisegger, F., Pfahl, S., Flamant, C., Lacour, J.-L. and Chaboureaud, J.-P.:
 1674 Contrasting stable water isotope signals from convective and large-scale precipitation
 1675 phases of a heavy precipitation event in southern Italy during HyMeX IOP 13: a modelling



1676 perspective, *Atmospheric Chemistry and Physics*, 19(11), 7487–7506, doi:10.5194/acp-
 1677 19-7487-2019, 2019.

1678

1679 Lindskog, M., Ridal, M., Thorsteinsson, S. and Ning, T.: Data assimilation of GNSS
 1680 zenith total delays from a Nordic processing centre, *Atmospheric Chemistry and Physics*,
 1681 17(22), 13983–13998, doi:10.5194/acp-17-13983-2017, 2017.

1682

1683 Llasat, M. C., Llasat-Botija, M., Prat, M. A., Porcú, F., Price, C., Mugnai, A., Lagouvardos,
 1684 K., Kotroni, V., Katsanos, D., Michaelides, S., Yair, Y., Savvidou, K. and Nicolaidis, K.:
 1685 High-impact floods and flash floods in Mediterranean countries: the FLASH preliminary
 1686 database, *Advances in Geosciences*, 23, 47–55, doi:10.5194/adgeo-23-47-2010, 2010.

1687

1688 Lovat, A., Vincendon, B. and Ducrocq, V.: Assessing the impact of resolution and soil
 1689 datasets on flash-flood modelling, *Hydrology and Earth System Sciences*, 23(3), 1801–
 1690 1818, doi:10.5194/hess-23-1801-2019, 2019.

1691

1692 Magnusson, L., Hewson, T. and Lavers, D.: Windstorm Alex affected large parts of
 1693 Europe, *ECMWF Newsletter*, 166, 4–5, 2021.

1694

1695 Maiello, I., Gentile, S., Ferretti, R., Baldini, L., Roberto, N., Picciotti, E., Alberoni, P. P.
 1696 and Marzano, F. S.: Impact of multiple radar reflectivity data assimilation on the
 1697 numerical simulation of a flash flood event during the HyMeX campaign, *Hydrology and*
 1698 *Earth System Sciences*, 21(11), 5459–5476, doi:10.5194/hess-21-5459-2017, 2017.

1699

1700 Manzato, A., Davolio, S., Miglietta, M. M., Pucillo, A. and Setvák, M.: 12 September
 1701 2012: A supercell outbreak in NE Italy?, *Atmospheric Research*, 153, 98–118,
 1702 doi:10.1016/j.atmosres.2014.07.019, 2015.

1703

1704 Mariotti, A.: Recent Changes in the Mediterranean Water Cycle: A Pathway toward Long-
 1705 Term Regional Hydroclimatic Change?, *Journal of Climate*, 23(6), 1513–1525,
 1706 doi:10.1175/2009jcli3251.1, 2010.

1707

1708 Marsigli, C., Montani, A. and Paccagnella, T.: Provision of boundary conditions for a
 1709 convection-permitting ensemble: comparison of two different approaches, *Nonlinear*
 1710 *Processes in Geophysics*, 21(2), 393–403, doi:10.5194/npg-21-393-2014, 2014.

1711



- 1712 Martinet, M., Nuissier, O., Duffourg, F., Ducrocq, V. and Ricard, D.: Fine-scale numerical
 1713 analysis of the sensitivity of the HyMeX IOP16a heavy precipitating event to the turbulent
 1714 mixing-length parametrization, *Quarterly Journal of the Royal Meteorological Society*,
 1715 143(709), 3122–3135, doi:10.1002/qj.3167, 2017.
- 1716
- 1717 Meroni, A. N., Parodi, A. and Pasquero, C.: Role of SST Patterns on Surface Wind
 1718 Modulation of a Heavy Midlatitude Precipitation Event, *Journal of Geophysical Research:*
 1719 *Atmospheres*, 123(17), 9081–9096, doi:10.1029/2018jd028276, 2018a.
- 1720
- 1721 Meroni, A. N., Renault, L., Parodi, A. and Pasquero, C.: Role of the Oceanic Vertical
 1722 Thermal Structure in the Modulation of Heavy Precipitations Over the Ligurian Sea, *Pure*
 1723 *and Applied Geophysics*, 175(11), 4111–4130, doi:10.1007/s00024-018-2002-y, 2018b.
- 1724
- 1725 Miglietta, M. M. and Rotunno, R.: Numerical Simulations of Conditionally Unstable Flows
 1726 over a Mountain Ridge, *Journal of the Atmospheric Sciences*, 66(7), 1865–1885,
 1727 doi:10.1175/2009jas2902.1, 2009.
- 1728
- 1729 Miglietta, M. M. and Rotunno, R.: Numerical Simulations of Sheared Conditionally
 1730 Unstable Flows over a Mountain Ridge, *Journal of the Atmospheric Sciences*, 71(5),
 1731 1747–1762, doi:10.1175/jas-d-13-0297.1, 2014.
- 1732
- 1733 Miglietta, M. M., Manzato, A. and Rotunno, R.: Characteristics and predictability of a
 1734 supercell during HyMeX SOP1, *Quarterly Journal of the Royal Meteorological Society*,
 1735 142(700), 2839–2853, doi:10.1002/qj.2872, 2016.
- 1736
- 1737 Moeng, C.-H., Sullivan, P. P., Khairoutdinov, M. F. and Randall, D. A.: A Mixed Scheme
 1738 for Subgrid-Scale Fluxes in Cloud-Resolving Models, *Journal of the Atmospheric*
 1739 *Sciences*, 67(11), 3692–3705, doi:10.1175/2010jas3565.1, 2010.
- 1740
- 1741 Molinié, G., Ceresetti, D., Anquetin, S., Creutin, J. D. and Boudevillain, B.: Rainfall
 1742 Regime of a Mountainous Mediterranean Region: Statistical Analysis at Short Time
 1743 Steps, *Journal of Applied Meteorology and Climatology*, 51(3), 429–448,
 1744 doi:10.1175/2011jamc2691.1, 2012.
- 1745
- 1746 Nelson, G. C., Rosegrant, M. W., Palazzo, A., Gray, I., Ingersoll, C., Robertson, R.,
 1747 Tokgoz, S., Zhu, T., Sulser, T. B., Ringler, C., Msangi, S. and You, L.: Food Security,



- 1748 Farming, and Climate Change to 2050: Scenarios, Results, Policy Options, International
 1749 Food Policy Research Institute., 2010.
- 1750
- 1751 Nielsen, E. R. and Schumacher, R. S.: Using Convection-Allowing Ensembles to
 1752 Understand the Predictability of an Extreme Rainfall Event, *Monthly Weather Review*,
 1753 144(10), 3651–3676, doi:10.1175/mwr-d-16-0083.1, 2016.
- 1754
- 1755 Nuissier, O., Ducrocq, V., Ricard, D., Lebeaupin, C. and Anquetin, S.: A numerical study
 1756 of three catastrophic precipitating events over southern France. I: Numerical framework
 1757 and synoptic ingredients, *Quarterly Journal of the Royal Meteorological Society*,
 1758 134(630), 111–130, doi:10.1002/qj.200, 2008.
- 1759
- 1760 Nuissier, O., Joly, B., Joly, A., Ducrocq, V. and Arbogast, P.: A statistical downscaling to
 1761 identify the large-scale circulation patterns associated with heavy precipitation events
 1762 over southern France, *Quarterly Journal of the Royal Meteorological Society*, 137(660),
 1763 1812–1827, doi:10.1002/qj.866, 2011.
- 1764
- 1765 Nuissier, O., Joly, B., Vié, B. and Ducrocq, V.: Uncertainty of lateral boundary conditions
 1766 in a convection-permitting ensemble: a strategy of selection for Mediterranean heavy
 1767 precipitation events, *Natural Hazards and Earth System Sciences*, 12(10), 2993–3011,
 1768 doi:10.5194/nhess-12-2993-2012, 2012.
- 1769
- 1770 Nuissier, O., Marsigli, C., Vincendon, B., Hally, A., Bouttier, F., Montani, A. and
 1771 Paccagnella, T.: Evaluation of two convection-permitting ensemble systems in the
 1772 HyMeX Special Observation Period (SOP1) framework, *Quarterly Journal of the Royal*
 1773 *Meteorological Society*, 142, 404–418, doi:10.1002/qj.2859, 2016.
- 1774
- 1775 Nuissier, O., Duffourg, F., Martinet, M., Ducrocq, V. and Lac, C.: Hectometric-scale
 1776 simulations of a Mediterranean heavy-precipitation event during the Hydrological cycle
 1777 in the Mediterranean Experiment (HyMeX) first Special Observation Period (SOP1),
 1778 *Atmospheric Chemistry and Physics*, 20(23), 14649–14667, doi:10.5194/acp-20-14649-
 1779 2020, 2020.
- 1780
- 1781 Oertel, A., Boettcher, M., Joos, H., Sprenger, M., Konow, H., Hagen, M. and Wernli, H.:
 1782 Convective activity in an extratropical cyclone and its warm conveyor belt – a case-study
 1783 combining observations and a convection-permitting model simulation, *Quarterly Journal*
 1784 *of the Royal Meteorological Society*, 145(721), 1406–1426, doi:10.1002/qj.3500, 2019.



- 1785 Oost, W. A., Komen, G. J., Jacobs, C. M. J. and Oort, C. V.: New evidence for a relation
 1786 between wind stress and wave age from measurements during ASGAMAGE, Boundary-
 1787 Layer Meteorology, 103(3), 409–438, doi:10.1023/a:1014913624535, 2002.
- 1788 Orłowsky, B. and Seneviratne, S. I.: Global changes in extreme events: regional and
 1789 seasonal dimension, Climatic Change, 110(3-4), 669–696, doi:10.1007/s10584-011-
 1790 0122-9, 2011.
- 1791
- 1792 Papagiannaki, K., Kotroni, V., Lagouvardos, K., Ruin, I. and Bezes, A.: Urban Area
 1793 Response to Flash Flood–Triggering Rainfall, Featuring Human Behavioral Factors: The
 1794 Case of 22 October 2015 in Attica, Greece, Weather, Climate, and Society, 9(3), 621–
 1795 638, doi:10.1175/wcas-d-16-0068.1, 2017.
- 1796
- 1797 Pfahl, S., Madonna, E., Boettcher, M., Joos, H. and Wernli, H.: Warm Conveyor Belts in
 1798 the ERA-Interim Dataset (1979–2010). Part II: Moisture Origin and Relevance for
 1799 Precipitation, Journal of Climate, 27(1), 27–40, doi:10.1175/jcli-d-13-00223.1, 2014.
- 1800 Pichelli, E., Rotunno, R. and Ferretti, R.: Effects of the Alps and Apennines on forecasts
 1801 for Po Valley convection in two HyMeX cases, Quarterly Journal of the Royal
 1802 Meteorological Society, 143(707), 2420–2435, doi:10.1002/qj.3096, 2017.
- 1803
- 1804 Planton, S., Driouech, F., Rhaz, K. E. and Lionello, P.: The climate of the Mediterranean
 1805 regions in the future climate projections. In: The Mediterranean region under climate
 1806 change, p.86., 2016.
- 1807
- 1808 Poletti, M. L., Silvestro, F., Davolio, S., Pignone, F. and Rebora, N.: Using nowcasting
 1809 technique and data assimilation in a meteorological model to improve very short range
 1810 hydrological forecasts, Hydrology and Earth System Sciences, 23(9), 3823–3841,
 1811 doi:10.5194/hess-23-3823-2019, 2019.
- 1812
- 1813 Prein, A. F., Langhans, W., Fosser, G., Ferrone, A., Ban, N., Goergen, K., Keller, M.,
 1814 Tölle, M., Gutjahr, O., Feser, F., Brisson, E., Kollet, S., Schmidli, J., Lipzig, N. P. M. and
 1815 Leung, R.: A review on regional convection-permitting climate modeling:
 1816 Demonstrations, prospects, and challenges, Reviews of Geophysics, 53(2), 323–361,
 1817 doi:10.1002/2014rg000475, 2015.
- 1818
- 1819 Protat, A., Bouniol, D., Delanoë, J., O'Connor, E., May, P. T., Plana-Fattori, A., Hasson,
 1820 A., Görsdorf, U. and Heymsfield, A. J.: Assessment of Cloudsat Reflectivity
 1821 Measurements and Ice Cloud Properties Using Ground-Based and Airborne Cloud



- 1822 Radar Observations, *Journal of Atmospheric and Oceanic Technology*, 26(9), 1717–
 1823 1741, doi:10.1175/2009jtecha1246.1, 2009.
- 1824
- 1825 Rainaud, R., Brossier, C. L., Ducrocq, V., Giordani, H., Nuret, M., Fourrié, N., Bouin, M.-
 1826 N., Taupier-Letage, I. and Legain, D.: Characterization of air-sea exchanges over the
 1827 Western Mediterranean Sea during HyMeX SOP1 using the AROME-WMED model,
 1828 *Quarterly Journal of the Royal Meteorological Society*, 142, 173–187,
 1829 doi:10.1002/qj.2480, 2015.
- 1830
- 1831 Rainaud, R., Brossier, C. L., Ducrocq, V. and Giordani, H.: High-resolution air-sea
 1832 coupling impact on two heavy precipitation events in the Western Mediterranean,
 1833 *Quarterly Journal of the Royal Meteorological Society*, 143(707), 2448–2462,
 1834 doi:10.1002/qj.3098, 2017.
- 1835
- 1836 Raupach, T. H. and Berne, A.: Small-Scale Variability of the Raindrop Size Distribution
 1837 and Its Effect on Areal Rainfall Retrieval, *Journal of Hydrometeorology*, 17(7), 2077–
 1838 2104, doi:10.1175/jhm-d-15-0214.1, 2016.
- 1839
- 1840 Ravazzani, G., Amengual, A., Ceppi, A., Homar, V., Romero, R., Lombardi, G. and
 1841 Mancini, M.: Potentialities of ensemble strategies for flood forecasting over the Milano
 1842 urban area, *Journal of Hydrology*, 539, 237–253, doi:10.1016/j.jhydrol.2016.05.023,
 1843 2016.
- 1844
- 1845 Raveh-Rubin, S. and Flaounas, E.: A dynamical link between deep Atlantic extratropical
 1846 cyclones and intense Mediterranean cyclones, *Atmospheric Science Letters*, 18(5), 215–
 1847 221, doi:10.1002/asl.745, 2017.
- 1848
- 1849 Raveh-Rubin, S. and Wernli, H.: Large-scale wind and precipitation extremes in the
 1850 Mediterranean: a climatological analysis for 1979-2012, *Quarterly Journal of the Royal*
 1851 *Meteorological Society*, 141(691), 2404–2417, doi:10.1002/qj.2531, 2015.
- 1852
- 1853 Raynaud, L. and Bouttier, F.: Comparison of initial perturbation methods for ensemble
 1854 prediction at convective scale, *Quarterly Journal of the Royal Meteorological Society*,
 1855 142(695), 854–866, doi:10.1002/qj.2686, 2015.
- 1856
- 1857 Rebora, N., Molini, L., Casella, E., Comellas, A., Fiori, E., Pignone, F., Siccardi, F.,
 1858 Silvestro, F., Tanelli, S. and Parodi, A.: Extreme Rainfall in the Mediterranean: What Can



- 1859 We Learn from Observations?, *Journal of Hydrometeorology*, 14(3), 906–922,
 1860 doi:10.1175/jhm-d-12-083.1, 2013.
- 1861
- 1862 Ribaud, J.-F., Bousquet, O., Coquillat, S., Al-Sakka, H., Lambert, D., Ducrocq, V. and
 1863 Fontaine, E.: Evaluation and application of hydrometeor classification algorithm outputs
 1864 inferred from multi-frequency dual-polarimetric radar observations collected during
 1865 HyMeX, *Quarterly Journal of the Royal Meteorological Society*, 142, 95–107,
 1866 doi:10.1002/qj.2589, 2015.
- 1867
- 1868 Ribaud, J.-F., Bousquet, O. and Coquillat, S.: Relationships between total lightning
 1869 activity, microphysics and kinematics during the 24 September 2012 HyMeX bow-echo
 1870 system, *Quarterly Journal of the Royal Meteorological Society*, 142, 298–309,
 1871 doi:10.1002/qj.2756, 2016.
- 1872
- 1873 Ricard, D., Ducrocq, V. and Auger, L.: A Climatology of the Mesoscale Environment
 1874 Associated with Heavily Precipitating Events over a Northwestern Mediterranean Area,
 1875 *Journal of Applied Meteorology and Climatology*, 51(3), 468–488, doi:10.1175/jamc-d-
 1876 11-017.1, 2012.
- 1877
- 1878 Richard, E., Buzzi, A. and Zängl, G.: Quantitative precipitation forecasting in the Alps:
 1879 The advances achieved by the Mesoscale Alpine Programme, *Quarterly Journal of the*
 1880 *Royal Meteorological Society*, 133(625), 831–846, doi:10.1002/qj.65, 2007.
- 1881
- 1882 Röhner, L., Nerding, K.-U. and Corsmeier, U.: Diagnostic study of a HyMeX heavy
 1883 precipitation event over Spain by investigation of moisture trajectories, *Quarterly Journal*
 1884 *of the Royal Meteorological Society*, 142, 287–297, doi:10.1002/qj.2825, 2016.
- 1885 Rolph, G., Stein, A. and Stunder, B.: Real-time Environmental Applications and Display
 1886 sYstem: READY, *Environmental Modelling & Software*, 95, 210–228,
 1887 doi:10.1016/j.envsoft.2017.06.025, 2017.
- 1888
- 1889 Romero, R., Ramis, C. and Homar, V.: On the severe convective storm of 29 October
 1890 2013 in the Balearic Islands: observational and numerical study, *Quarterly Journal of the*
 1891 *Royal Meteorological Society*, 141(689), 1208–1222, doi:10.1002/qj.2429, 2014.
- 1892 Roux, H., Amengual, A., Romero, R., Bladé, E. and Sanz-Ramos, M.: Evaluation of two
 1893 hydrometeorological ensemble strategies for flash-flood forecasting over a catchment of
 1894 the eastern Pyrenees, *Natural Hazards and Earth System Sciences*, 20(2), 425–450,
 1895 doi:10.5194/nhess-20-425-2020, 2020.



- 1896
- 1897 Ruin, I., Lutoff, C., Boudevillain, B., Creutin, J.-D., Anquetin, S., Rojo, M. B., Boissier, L.,
- 1898 Bonnifait, L., Borga, M., Colbeau-Justin, L., Creton-Cazanave, L., Delrieu, G., Douvinet,
- 1899 J., Gaume, E., Gruntfest, E., Naulin, J.-P., Payrastre, O. and Vannier, O.: Social and
- 1900 Hydrological Responses to Extreme Precipitations: An Interdisciplinary Strategy for
- 1901 Postflood Investigation, *Weather, Climate, and Society*, 6(1), 135–153,
- 1902 doi:10.1175/wcas-d-13-00009.1, 2014.
- 1903
- 1904 Sauvage, C., Brossier, C. L., Bouin, M.-N. and Ducrocq, V.: Characterization of the air–
- 1905 sea exchange mechanisms during a Mediterranean heavy precipitation event using
- 1906 realistic sea state modelling, *Atmospheric Chemistry and Physics*, 20(3), 1675–1699,
- 1907 doi:10.5194/acp-20-1675-2020, 2020.
- 1908
- 1909 Scheffknecht, P., Richard, E. and Lambert, D.: A highly localized high-precipitation event
- 1910 over Corsica, *Quarterly Journal of the Royal Meteorological Society*, 142, 206–221,
- 1911 doi:10.1002/qj.2795, 2016.
- 1912
- 1913 Scheffknecht, P., Richard, E. and Lambert, D.: Climatology of heavy precipitation over
- 1914 Corsica in the period 1985–2015, *Quarterly Journal of the Royal Meteorological Society*,
- 1915 143(709), 2987–2998, doi:10.1002/qj.3140, 2017.
- 1916
- 1917 Schleiss, M. and Smith, J.: A Method to Estimate the 3D–Time Structure of the Raindrop
- 1918 Size Distribution Using Radar and Disdrometer Data*, *Journal of Hydrometeorology*,
- 1919 16(3), 1222–1242, doi:10.1175/jhm-d-14-0182.1, 2015.
- 1920
- 1921 Schumacher, R. S. and Johnson, R. H.: Organization and Environmental Properties of
- 1922 Extreme-Rain-Producing Mesoscale Convective Systems, *Monthly Weather Review*,
- 1923 133(4), 961–976, doi:10.1175/mwr2899.1, 2005.
- 1924
- 1925 Senatore, A., Davolio, S., Furnari, L. and Mendicino, G.: Reconstructing Flood Events in
- 1926 Mediterranean Coastal Areas Using Different Reanalyses and High-Resolution
- 1927 Meteorological Models, *Journal of Hydrometeorology*, 21(8), 1865–1887,
- 1928 doi:10.1175/jhm-d-19-0270.1, 2020a.
- 1929
- 1930 Senatore, A., Furnari, L. and Mendicino, G.: Impact of high-resolution sea surface
- 1931 temperature representation on the forecast of small Mediterranean catchments



- 1932 hydrological responses to heavy precipitation, *Hydrology and Earth System Sciences*,
 1933 24(1), 269–291, doi:10.5194/hess-24-269-2020, 2020b.
- 1934
- 1935 Seyfried, L., Estournel, C., Marsaleix, P. and Richard, E.: Dynamics of North Balearic
 1936 Front during an autumn Tramontane and Mistral storm: air–sea coupling processes and
 1937 stratification budget diagnostic, doi:10.5194/os-2018-14, 2018.
- 1938
- 1939 Sodemann, H., Aemisegger, F., Pfahl, S., Bitter, M., Corsmeier, U., Feuerle, T., Graf, P.,
 1940 Hankers, R., Hsiao, G., Schulz, H., Wieser, A. and Wernli, H.: The stable isotopic
 1941 composition of water vapour above Corsica during the HyMeX SOP1 campaign: insight
 1942 into vertical mixing processes from lower-tropospheric survey flights, *Atmospheric*
 1943 *Chemistry and Physics*, 17(9), 6125–6151, doi:10.5194/acp-17-6125-2017, 2017.
- 1944
- 1945 Stein, A. F., Draxler, R. R., Rolph, G. D., Stunder, B. J. B., Cohen, M. D. and Ngan, F.:
 1946 NOAA's HYSPLIT Atmospheric Transport and Dispersion Modeling System, *Bulletin of*
 1947 *the American Meteorological Society*, 96(12), 2059–2077, doi:10.1175/bams-d-14-
 1948 00110.1, 2015.
- 1949
- 1950 Stocchi, P. and Davolio, S.: Intense air-sea exchanges and heavy orographic
 1951 precipitation over Italy: The role of Adriatic sea surface temperature uncertainty,
 1952 *Atmospheric Research*, 196, 62–82, doi:10.1016/j.atmosres.2017.06.004, 2017.
- 1953
- 1954 Strajnar, B., Cedilnik, J., Fettich, A., Ličer, M., Pristov, N., Smerkol, P. and Jerman, J.:
 1955 Impact of two-way coupling and sea-surface temperature on precipitation forecasts in
 1956 regional atmosphere and ocean models, *Quarterly Journal of the Royal Meteorological*
 1957 *Society*, 145(718), 228–242, doi:10.1002/qj.3425, 2019.
- 1958
- 1959 Strauss, C., Ricard, D., Lac, C. and Verrelle, A.: Evaluation of turbulence
 1960 parametrizations in convective clouds and their environment based on a large-eddy
 1961 simulation, *Quarterly Journal of the Royal Meteorological Society*, 145(724), 3195–3217,
 1962 doi:10.1002/qj.3614, 2019.
- 1963
- 1964 Taufour, M., Vié, B., Augros, C., Boudevillain, B., Delanoë, J., Delautier, G., Ducrocq,
 1965 V., Lac, C., Pinty, J.-P. and Schwarzenböck, A.: Evaluation of the two-moment scheme
 1966 LIMA based on microphysical observations from the HyMeX campaign, *Quarterly*
 1967 *Journal of the Royal Meteorological Society*, 144(714), 1398–1414, doi:10.1002/qj.3283,
 1968 2018.



- 1969
- 1970 Thévenot, O., Bouin, M.-N., Ducrocq, V., Brossier, C. L., Nuissier, O., Pianezze, J. and
- 1971 Duffourg, F.: Influence of the sea state on Mediterranean heavy precipitation: a case-
- 1972 study from HyMeX SOP1, Quarterly Journal of the Royal Meteorological Society, 142,
- 1973 377–389, doi:10.1002/qj.2660, 2015.
- 1974
- 1975 Trambly, Y. and Somot, S.: Future evolution of extreme precipitation in the
- 1976 Mediterranean, Climatic Change, 151(2), 289–302, doi:10.1007/s10584-018-2300-5,
- 1977 2018.
- 1978
- 1979 Turato, B., Reale, O. and Siccardi, F.: Water Vapor Sources of the October 2000
- 1980 Piedmont Flood, Journal of Hydrometeorology, 5(4), 693–712, doi:10.1175/1525-
- 1981 7541(2004)005<0693:wvsoto>2.0.co;2, 2004.
- 1982
- 1983 Uber, M., Vandervaere, J.-P., Zin, I., Braud, I., Heistermann, M., Legout, C., Molinié, G.
- 1984 and Nord, G.: How does initial soil moisture influence the hydrological response? A case
- 1985 study from southern France, Hydrology and Earth System Sciences, 22(12), 6127–6146,
- 1986 doi:10.5194/hess-22-6127-2018, 2018.
- 1987
- 1988 Varble, A., Fridlind, A. M., Zipser, E. J., Ackerman, A. S., Chaboureau, J.-P., Fan, J., Hill,
- 1989 A., McFarlane, S. A., Pinty, J.-P. and Shipway, B.: Evaluation of cloud-resolving model
- 1990 intercomparison simulations using TWP-ICE observations: Precipitation and cloud
- 1991 structure, Journal of Geophysical Research, 116(D12), doi:10.1029/2010jd015180,
- 1992 2011.
- 1993
- 1994 Verrelle, A., Ricard, D. and Lac, C.: Sensitivity of high-resolution idealized simulations of
- 1995 thunderstorms to horizontal resolution and turbulence parametrization, Quarterly Journal
- 1996 of the Royal Meteorological Society, 141(687), 433–448, doi:10.1002/qj.2363, 2014.
- 1997 Verrelle, A., Ricard, D. and Lac, C.: Evaluation and Improvement of Turbulence
- 1998 Parameterization inside Deep Convective Clouds at Kilometer-Scale Resolution,
- 1999 Monthly Weather Review, 145(10), 3947–3967, doi:10.1175/mwr-d-16-0404.1, 2017.
- 2000
- 2001 Vié, B., Molinié, G., Nuissier, O., Vincendon, B., Ducrocq, V., Bouttier, F. and Richard,
- 2002 E.: Hydro-meteorological evaluation of a convection-permitting ensemble prediction
- 2003 system for Mediterranean heavy precipitating events, Natural Hazards and Earth System
- 2004 Sciences, 12(8), 2631–2645, doi:10.5194/nhess-12-2631-2012, 2012.
- 2005



- 2006 Vié, B., Pinty, J.-P., Berthet, S. and Leriche, M.: LIMA (v1.0): A quasi two-moment
 2007 microphysical scheme driven by a multimodal population of cloud condensation and ice
 2008 freezing nuclei, *Geoscientific Model Development*, 9(2), 567–586, doi:10.5194/gmd-9-
 2009 567-2016, 2016.
- 2010
- 2011 Vincendon, B., Ducrocq, V., Nuissier, O. and Vié, B.: Perturbation of convection-
 2012 permitting NWP forecasts for flash-flood ensemble forecasting, *Natural Hazards and*
 2013 *Earth System Sciences*, 11(5), 1529–1544, doi:10.5194/nhess-11-1529-2011, 2011.
- 2014
- 2015 Winschall, A., Pfahl, S., Sodemann, H. and Wernli, H.: Impact of North Atlantic
 2016 evaporation hot spots on southern Alpine heavy precipitation events, *Quarterly Journal*
 2017 *of the Royal Meteorological Society*, 138(666), 1245–1258, doi:10.1002/qj.987, 2011.
- 2018 Wu, F., Cui, X. and Zhang, D.-L.: A lightning-based nowcast-warning approach for short-
 2019 duration rainfall events: Development and testing over Beijing during the warm seasons
 2020 of 2006–2007, *Atmospheric Research*, 205, 2–17, doi:10.1016/j.atmosres.2018.02.003,
 2021 2018.
- 2022
- 2023 Wyngaard, J. C. and Coté, O. R.: The Budgets of Turbulent Kinetic Energy and
 2024 Temperature Variance in the Atmospheric Surface Layer, *Journal of the Atmospheric*
 2025 *Sciences*, 28(2), 190–201, doi:10.1175/1520-0469(1971)028<0190:tbotke>2.0.co;2,
 2026 1971.
- 2027
- 2028 Xie, S.-P., Xu, H., Kessler, W. S. and Nonaka, M.: Air–Sea Interaction over the Eastern
 2029 Pacific Warm Pool: Gap Winds, Thermocline Dome, and Atmospheric Convection*,
 2030 *Journal of Climate*, 18(1), 5–20, doi:10.1175/jcli-3249.1, 2005.
- 2031
- 2032 Ziv, B., Saaroni, H., Romem, M., Heifetz, E., Harnik, N. and Baharad, A.: Analysis of
 2033 conveyor belts in winter Mediterranean cyclones, *Theoretical and Applied Climatology*,
 2034 99(3-4), 441–455, doi:10.1007/s00704-009-0150-9, 2009.
- 2035
- 2036 Zwiebel, J., Baelen, J. V., Anquetin, S., Pointin, Y. and Boudevillain, B.: Impacts of
 2037 orography and rain intensity on rainfall structure. The case of the HyMeX IOP7a event,
 2038 *Quarterly Journal of the Royal Meteorological Society*, 142, 310–319,
 2039 doi:10.1002/qj.2679, 2015.
- 2040